博士学位論文

腸管バリアの破綻に伴い、膵臓に定着する *Staphylococcus sciuri* が自己免疫性膵炎を悪化させる

近畿大学大学院
医学研究科医学系専攻
平井　智恵

Doctoral Dissertation

Disruption of the intestinal barrier exacerbates experimental autoimmune pancreatitis by promoting the translocation of *Staphylococcus sciuri* into the pancreas

November 2022

Major in Medical Sciences
Kindai University Graduate School of Medical Sciences

Tomoe Hirai

課博

同　意　書

2022 年　9月　6日

近畿大学大学院
医学研究科長　殿

共著者　二見芳輔　印　　共著者　大塚有生　印

共著者　原西　印　　共著者　高田雄太郎　印

共著者　瀬海有那衣　印　　共著者　鍔田研　印

共著者　栗田真之　印　　共著者　朴雅美　印

共著者　益田康弘　印　　共著者　高村果祝　印

論文題目

Disruption of the intestinal barrier exacerbates experimental autoimmune pancreatitis by promoting the translocation of Staphylococcus sciuri into the pancreas

下記の博士論文提出者が、標記論文を貴学医学博士の学位論文（主論文）として使用することに同意いたします。

また、標記論文を再び学位論文として使用しないことを誓約いたします。

記

1．博士論文提出者氏名　　平井　智恵

2．専攻分野　　医学系　　消化器病態制御学

課博

同　意　書

2022年　9月　6日

近畿大学大学院
医学研究科長　殿

共著者　工藤正俊　㊞　　共著者　＿＿＿＿＿＿＿＿　㊞

共著者　渡邊智裕　㊞　　共著者　＿＿＿＿＿＿＿＿　㊞

共著者　＿＿＿＿＿＿＿＿　㊞　　共著者　＿＿＿＿＿＿＿＿　㊞

共著者　＿＿＿＿＿＿＿＿　㊞　　共著者　＿＿＿＿＿＿＿＿　㊞

共著者　＿＿＿＿＿＿＿＿　㊞　　共著者　＿＿＿＿＿＿＿＿　㊞

論文題目

Disruption of the intestinal barrier exacerbates experimental autoimmune pancreatitis by promoting the translocation of Staphylococcus sciuri into the pancreas

下記の博士論文提出者が、標記論文を貴学医学博士の学位論文（主論文）として使用することに同意いたします。

また、標記論文を再び学位論文として使用しないことを誓約いたします。

記

1．博士論文提出者氏名　　平井　智恵

2．専攻分野　　医学系　　消化器病態制御学

Disruption of Intestinal Barrier Exacerbates Experimental Autoimmune Pancreatitis by Promoting Translocation of *Staphylococcus sciuri* into Pancreas

Running title: Gut-pancreas axis in autoimmune pancreatitis

Tomoe Yoshikawa[1], Kosuke Minaga[1], Akane Hara[1], Ikue Sekai[1], Masayuki Kurimoto[1], Yasuhiro Masuta[1], Yasuo Otsuka[1], Ryutaro Takada[1], Ken Kamata[1], Ah-Mee Park[2], Shiki Takamura[3], Masatoshi Kudo[1], Tomohiro Watanabe[1]

[1]Department of Gastroenterology and Hepatology, Kindai University Faculty of Medicine, 377-2 Ohno-Higashi, Osaka-Sayama, Osaka 589-8511, Japan

[2]Department of Microbiology, Kindai University Faculty of Medicine,

377-2 Ohno-Higashi, Osaka-Sayama, Osaka 589-8511, Japan

[3]Department of Immunology, Kindai University Faculty of Medicine,

377-2 Ohno-Higashi, Osaka-Sayama, Osaka 589-8511, Japan

Correspondence to: Tomohiro Watanabe, MD, PhD.

Department of Gatsroenterology and Hepatology, Kindai University Faculty of Medicine,

377-2 Ohno-Higashi, Osaka-Sayama, Osaka 589-8511, Japan,

Phone: +81-72-366-0221, Fax: +81-72-367-2880

Email: tomohiro@med.kindai.ac.jp

Abstract

Autoimmune pancreatitis (AIP) and IgG4-related disease (IgG4-RD) are new disease entities characterized by enhanced IgG4 antibody (Ab) responses and involvement of multiple organs, including the pancreas and salivary glands. Although the immunopathogenesis of AIP and IgG4-RD is poorly understood, we previously reported that intestinal dysbiosis mediates experimental AIP through the activation of IFN-α- and IL-33-producing plasmacytoid dendritic cells (pDCs). Because intestinal dysbiosis is linked to intestinal barrier dysfunction, we explored whether the latter affects the development of AIP and autoimmune sialadenitis in MRL/MpJ mice treated with repeated injections of polyinosinic-polycytidylic acid (poly (I:C)). Epithelial barrier disruption was induced by the administration of dextran sodium sulfate (DSS) in the drinking water. Mice co-treated with poly (I:C) and DSS, but not those treated with either agent alone, developed severe AIP, but not autoimmune sialadenitis, which was accompanied by the increased accumulation of IFN-α- and IL-33-producing pDCs. Sequencing of 16S ribosomal RNA revealed that *Staphylococcus sciuri* translocation from the gut to the pancreas was preferentially observed in mice with severe AIP co-treated with DSS and poly (I:C). The degree of experimental AIP, but not of autoimmune sialadenitis, was greater in germ-free mice mono-colonized with *S. sciuri* and treated with poly (I:C) than in germ-free mice treated with poly (I:C) alone, which was accompanied by the increased accumulation of IFN-α- and IL-33-producing pDCs. Taken together, these data suggest that intestinal barrier dysfunction exacerbates AIP through the activation of pDCs and translocation of *S. sciuri* into the pancreas.

Keywords: Plasmacytoid dendritic cells, Autoimmune pancreatitis, Autoimmune sialadenitis, Intestinal barrier, *Staphylococcus sciuri*

Abbreviations used in this article: Ab, antibody; AIP, autoimmune pancreatitis; BHI, brain heart infusion; CFU, colony forming unit; DSS, dextran sodium sulfate; ELISA, enzyme-linked immunosorbent assay; GF, germ-free; GI, gastrointestinal; H&E, hematoxylin and eosin; IgG4-RD, IgG4-related disease; IP, intraperitoneal; NOD2, nucleotide-binding oligomerization domain 2; pDC, plasmacytoid dendritic cell; PCoA, Principal-coordinate analysis; PDCA, pDC antigen; poly (I:C), polyinosinic-polycytidylic acid; ribosomal RNA, rRNA; Toll-like receptor, TLR.

Introduction

Autoimmune pancreatitis (AIP) is classified as type 1 and type 2, the former of which is a pancreatic manifestation of systemic IgG4-related disease (IgG4-RD) (1-4). More than 95% of AIP cases are classified as type 1 AIP (1-4). Hereafter, type 1 AIP is simply referred to as 'AIP'. AIP and IgG4-RD are characterized by elevated serum concentrations of IgG4 antibody (Ab) and accumulation of IgG4-expressing plasma cells in the affected organs (1-4). Another prominent feature of AIP and IgG4-RD is multiple organ involvement (1-4). These autoimmune disorders preferentially target the pancreas, bile duct, kidneys, and salivary glands (1-4). Although previous studies addressing the immunopathogenesis of AIP and IgG4-RD have focused on immune reactions responsible for enhanced IgG4 Ab responses, few studies have explored the molecular mechanisms accounting for the development of multiple organ involvement. Recently, we found that the activation of plasmacytoid dendritic cells (pDCs) followed by enhanced IFN-α and IL-33 responses is a prominent feature of experimental AIP and human IgG4-RD (4-9). In subsequent studies, we provided evidence that intestinal dysbiosis mediates the development of experimental and human AIP (6,10). However, it remains largely unknown whether intestinal dysbiosis affects the development of multiple organ damage, especially of the extra-pancreatic inflammation seen in individuals with AIP and IgG4-RD.

Leaky gut syndrome, a condition of increased intestinal epithelial permeability, attracts much attention because it permits environmental and microbial factors to enter the body, thereby triggering inflammatory responses not only in the gastrointestinal (GI) tract but also in extra-GI organs (11-15). Growing evidence suggests that the intestinal microbiota

plays an important role in the maintenance of gut epithelial barrier integrity, whereas intestinal dysbiosis disrupts the epithelial barrier (11-15). Importantly, leaky gut and intestinal dysbiosis are associated with the development of autoimmune diseases of extra-GI organs, cardiometabolic disease, and aging-related inflammation (11-15). Thus, it is well established that intestinal barrier dysfunction and gut dysbiosis underlie the pathogenesis of various human extra-GI disorders. Most patients with AIP and IgG4-RD are elderly men (1-4). Given that epithelial barrier integrity is often impaired in the elderly, it is likely that increased intestinal epithelial permeability caused by the presence of leaky gut can initiate AIP and autoimmune sialadenitis, both of which are prototypical autoimmune disorders associated with IgG4-RD. In addition, as shown in our previous studies, intestinal dysbiosis mediates experimental AIP via the activation of pDCs (6,10). Based on these findings, we hypothesized that the disruption of the intestinal barrier function and intestinal dysbiosis act together to promote chronic fibroinflammatory responses in the pancreas and extra-pancreatic organs of AIP and IgG4-RD. To address this question, we utilized a well-established experimental model of AIP and autoimmune sialadenitis induced in MRL/MpJ mice by repeated injections of polyinosinic-polycytidylic acid (poly (I:C)) (16). Here, we provide evidence that disruption of the intestinal barrier by dextran sodium sulfate (DSS) exacerbates poly (I:C)-induced experimental AIP, but not autoimmune sialadenitis, through the activation of IFN-α- and IL-33-producing pDCs. We also show that experimental AIP exacerbation by the disruption of the epithelial barrier was associated with the translocation of *Staphylococcus sciuri* into the pancreas.

Materials and Methods

Experimental animals and treatments

Female MRL/MpJ mice were obtained from Japan SLC (Hamamatsu, Japan) and maintained in the Kindai University animal facility under specific pathogen-free conditions. The study protocol for animal experiments was approved by the Review Board of the Kindai University Faculty of Medicine. Six-week-old female MRL/MpJ mice received intraperitoneal (IP) injections of 100 μg of poly (I:C) (InvivoGen, San Diego, CA) two or three times a week for a total of 15 times to induce experimental AIP, as previously described (5,9). MRI/MpJ mice were also treated with 2% DSS in the drinking water every two weeks to disrupt the intestinal barrier function (17,18). To determine the effect of intestinal barrier dysfunction on the development of AIP, MRL/MpJ mice received both poly (I:C) and DSS treatments (Fig. 1A). In some experiments, MRL/MpJ mice were treated with 120G8 Ab (BioXcell, Lebanon, NH) or control rat IgG (Sigma-Aldrich, St. Louis, MO) as previously described (5). Mice received IP injection of Ab prior to each poly (I:C) injection (0.1 mg/each mouse).

Generation of germ-free mice and gnotobiotic mice

Germ-free (GF) MRL/MpJ mice were created in SLC, as previously described (19-21). GF female 10–13-week-old MRL/MpJ mice were housed in the animal facility of the Kindai University Faculty of Medicine, in accordance with previous reports (19-21). Gnotobiotic MRL/MpJ mice were created in SLC, as previously described (19-21). Colonization of GF mice with *S. sciuri* was performed by SLC and confirmed by stool culture. GF mice and gnotobiotic mice colonized with *S. sciuri* were treated with a total

of 16 IP injections of 10 μg of poly (I:C) to induce mild AIP, as previously described (6,10).

Preparation of bacteria

S. sciuri was obtained from Riken BRC (JCM#2425, Ibaraki, Japan) and cultured in brain heart infusion (BHI) broth (Eiken Chemical Co., Ltd., Tochigi, Japan) at 37 °C. The number of bacteria in the suspension was optically determined at 600 nm. The optical density of 0.33 corresponded to a concentration of approximately 10^8 colony forming unit (CFU)/mL. A 2×10^9 CFU/mL suspension of *S. sciuri* in BHI broth containing 20% glycerol was aliquoted into 1.5 mL microtubes and stored at −80 °C until use. After thawing and culturing on BHI agar medium, more than 95% of the bacteria were confirmed to be viable. *Bifidobacterium pseudolongum* and *Klebsiella pneumoniae* were prepared as previously described (6,10). *Staphylococcus aureus* was obtained from ATCC (Manassas, VA) and cultured in BHI broth. The optical density of 0.28 at 600 nm corresponded to a concentration of approximately 10^8 CFU/mL.

Histological analyses

Samples were obtained from the pancreas, salivary glands, and colon of MRL/MpJ mice that were sacrificed 3 h after the final injection of poly (I:C). These samples were fixed with 10% formalin and stained with hematoxylin and eosin (H&E). Pathological assessment was performed using a scoring system for AIP, autoimmune sialadenitis, and colitis, in accordance with previous reports (5,9,17,18,22,23). Pancreatic inflammation was scored as follows: 0, pancreas without mononuclear cell infiltration; 1, mononuclear cell aggregation and/or infiltration within the interstitium with no parenchymal destruction; 2, focal parenchymal destruction with mononuclear cell infiltration; 3,

diffuse parenchymal destruction with some parenchymal areas remaining intact; and 4, almost all pancreatic tissue, except for pancreatic islets, destroyed or replaced with fibrotic or adipose tissue (5,9). Salivary gland inflammation was scored on a scale of 0–3 as follows: 0, normal; 1, mononuclear cell infiltration localized in periductular regions; 2, destruction of ductules with cell infiltration extending to the parenchyma; and 3, grade 2 changes plus proliferation of the residual ductules, granulomatous lesions, and/or fibrosis in the parenchyma (22,23). Histological samples were scored for DSS colitis as previously described (17,18). Epithelial injury was scored as follows: 0, normal morphology; 1, loss of goblet cells; 2, loss of goblet cells in large areas; 3, loss of crypts; and 4, loss of crypts in large areas. Immune cell infiltration was scored as follows: 0, no infiltrate; 1, infiltrate around crypt basis; 2, infiltrate reaching the lamina muscularis mucosae; 3, extensive infiltration reaching the lamina muscularis mucosae and thickening of the mucosae with abundant edema; and 4, infiltration of the lamina submucosa. The total histological score was given as a sum of the epithelial injury and infiltration scores. At least two H&E staining photographs were captured using a microscope (Biozero, BZ-8100, Keyence, Osaka, Japan) from each slide.

Cytokine assays

Cytokine concentrations in the pancreas, salivary glands, and colon were measured by the enzyme-linked immunosorbent assay (ELISA), as previously described (18,24). IFN-α and IL-33 concentrations were determined using ELISA kits from R&D Systems (Minneapolis, MN) and eBioscience (San Diego, CA), respectively.

Isolation of mononuclear cells from the pancreas, salivary glands, and colon

Pancreatic mononuclear cells, colonic lamina propria mononuclear cells, and salivary gland mononuclear cells were prepared from MRL/MpJ mice in accordance with previous reports (5,6,17,18). FITC- or PE-conjugated anti-B220 Ab (eBioscience), anti-pDC antigen (PDCA)-1 Ab (eBioscience), and anti-CD3 Ab (eBioscience) were used to determine the proportions of immune cells. Flow-cytometry analysis was performed using an Accuri C6 flow cytometer (BD Biosciences, San Jose, CA) and CFlow Plus software (BD Biosciences). In some experiments, pDCs were isolated from the pancreas of MRL/MpJ mice treated with poly (I:C) and/or DSS. pDCs, which were identified as PDCA-$1^{+}B220^{low}$ cells, were FACS-sorted by BD FACSAria (BD Biosciences). Pancreatic mononuclear cells were stained with PerCP/Cy5.5-conjugated anti-CD3 Ab (TONBO Biosciences, San Diego, CA), FITC-conjugated anti-B220 Ab (eBioscience), and APC-conjugated anti-PDCA-1 Ab (BioLegend, San Diego, CA). FACS-sorted pDCs ($5x10^5$/mL) were stimulated with heat-killed *B. pseudolongum*, *S. sciuri*, *S. aureus,* and *K. pneumoniae* for 48 hrs at the indicated doses as previously described (6,10). Culture supernatants were subjected to cytokine assays.

Fecal and pancreatic microbiota analysis

Fecal and pancreatic samples were collected from mice, and DNA was extracted using QIAamp DNA stool and tissue kits (Qiagen, Hilden, Germany) as previously described (6,10,25,26). 16S ribosomal RNA (16S rRNA) gene profiling with an Illumina library targeting the V3–V4 region was performed using DNA samples isolated from the stools and pancreas. The MiSeq system was used for 16S rRNA sequencing. Sequence data were processed using Trimmomatic, Cutadapt, and Fastq-join programs, and the obtained bacterial sequences were clustered into operational taxonomic units. The resulting

bacterial sequences were aligned with the Greengenes microbial gene database with 97% sequence similarity in QIIME (1.8.0) (6,10,25-27) .

Species richness, alpha diversity, and beta diversity were calculated as previously described (6,10,25-27). Differences in beta diversity were visualized in three-dimensional plots obtained by Principal-coordinate analysis (PCoA) (6,10,25-27). Differential abundance analysis at the species levels was performed using R package ALDEx2 (27,28). False discovery rate-corrected *P* values (Welch's t test) were calculated as per the Benjamini-Hochberg procedure (27,28). Effect size was determined by aldex.glm.effect. $P<0.05$ or Effect size >1 was considered as significant.

Quantification of pancreatic bacteria

DNA from the pancreas was extracted using QIAamp DNA tissue kits (Qiagen). Isolated DNA samples (10 ng/μL) were subjected to quantitative PCR analyses using primers targeting V3-V4 region (18). Ileal samples from non-treated MRL/MpJ mice were used as reference expression of 16S rRNA.

Statistical analysis

Statistical analysis was performed using Prism (GraphPad Software Inc., La Jolla, CA) as described previously (8). Mann-Whitney U test, which is a nonparametric version of unpaired t test, was used to evaluate the differences between two groups. For multiple comparison test, Kruskal-Wallis test, which is a nonparametric version of one-way ANOVA, was used to evaluate the differences. For post hoc analysis, the Bonferroni corrected Mann-Whitney U test was performed for comparison between two groups,

where each *P*-value was derived by multiplying a *P*-value derived by the number of tests. Effects were considered statistically significant for $P < 0.05$.

Results

Disruption of the intestinal barrier by DSS exacerbates AIP, but not autoimmune sialadenitis

Although multiple organs become damaged simultaneously and asynchronously in patients with AIP and IgG4-RD, the molecular mechanisms accounting for the development of multiple organ involvement remain unknown. We previously demonstrated that intestinal dysbiosis underlies the immunopathogenesis of AIP and IgG4-RD (6,10). In this study, we hypothesized that intestinal dysbiosis mediates the development of both AIP and autoimmune sialadenitis, the latter of which is a prototypical extra-pancreatic manifestation of IgG4-RD. It is well established that intestinal barrier dysfunction promotes intestinal dysbiosis, followed by the translocation of gut microbiota into extra-GI tissues (14,29,30). Administration of DSS in the drinking water causes disruption of the intestinal epithelial barrier (17,18,31). To address the relationship between the intestinal barrier function and pancreatic and extra-pancreatic inflammation, MRL/MpJ mice were treated with 2% DSS in the drinking water in combination with repeated IP injections of poly (I:C). As shown in Fig. 1A, four groups of experimental mice were utilized: i) control untreated mice, ii) mice that were treated with DSS in the drinking water every 2 weeks to disrupt the intestinal barrier, iii) mice that received IP injections of poly (I:C) two or three times a week for a total of 15 times to induce AIP, and iv) mice that received both DSS to disrupt the intestinal barrier and poly (I:C) to induce AIP. As expected, repeated IP injections of poly (I:C) resulted in the development of AIP characterized by the destruction of the pancreatic acinar architecture and accumulation of immune cells (Fig. 1B). Interestingly, the severity of AIP was significantly greater in mice treated with both DSS and poly (I:C) than in those treated

with poly (I:C) alone. DSS treatment did not induce AIP development. Semi-quantitative assessment of AIP by pathological scores also confirmed the development of severe AIP in mice treated with a combination of DSS and poly (I:C) as compared to the histological characteristics in the other three groups of mice (Fig. 1C).

We then turned our attention to the development of autoimmune sialadenitis, another autoimmune-driven disorder associated with AIP and IgG4-RD. As shown in Fig. 1B and 1C, the severity of autoimmune sialadenitis was similar in mice treated with poly (I:C) and in those treated with both DSS and poly (I:C). DSS treatment alone did not induce autoimmune sialadenitis. Finally, DSS treatment resulted in the development of colitis, the severity of which was not affected by the combined treatment with poly (I:C) (Fig. 1B and 1C). Thus, the intestinal barrier dysfunction induced by DSS exacerbated AIP, but not autoimmune sialadenitis.

Combined treatment with DSS and poly (I:C) induces pancreatic accumulation of IFN-α- and IL-33-producing pDCs

IFN-α- and IL-33-producing pDCs play pathogenic roles in the development of AIP in MRL/MpJ mice treated with repeated injections of poly (I:C) (4-10). Having found that treatment with both DSS and poly (I:C) led to the development of severe AIP, we explored whether pancreatic accumulation of pDCs was enhanced by co-treatment with the two agents. As shown in Fig. 2A, the percentage and number of pDCs, defined as PDCA-1^{+}B220^{low} cells by flow-cytometry analysis, were higher, although not significant, in the pancreas of mice treated with poly (I:C) alone as compared with those in untreated mice and in mice treated with DSS alone (Fig. 2A and 2C). Interestingly, the percentage

and number of pDCs were significantly higher in the pancreas of mice treated with both DSS and poly (I:C) than in those treated with poly (I:C) alone (Fig. 2A and 2C). DSS treatment alone did not induce pancreatic accumulation of pDCs. Induction of AIP by poly (I:C) was accompanied by increased infiltration of $CD3^+$ T cells in the pancreas compared to their number after DSS treatment (Fig. 2B and 2C). The combined treatment with DSS and poly (I:C) did not alter the percentages of $CD3^+$ T cells or $B220^+$ B cells in the pancreas as compared with those in mice treated with poly (I:C) alone (Fig. 2B and 2C). In line with the enhanced accumulation of pDCs in the pancreas, pancreatic expression levels of IFN-α and IL-33 were higher in mice treated with both DSS and poly (I:C) than in those treated with poly (I:C) alone (Fig. 2D). These data suggest that intestinal barrier dysfunction induced by DSS promoted pancreatic accumulation of pDCs producing both IFN-α and IL-33, thereby aggravating AIP in MRL/MpJ mice.

Combined treatment with DSS and poly (I:C) induces colonic accumulation of IFN-α- and IL-33-producing pDCs

Next, we examined whether the colon and pancreas share pathogenic immune responses upon exposure to DSS and poly (I:C). Consistent with the results obtained in the pancreas, the percentage of pDCs was higher in the colon of mice treated with poly (I:C) alone as compared with those treated with DSS alone (Supplementary Fig. 1A and 1C). Interestingly, the proportion of pDCs in the colonic mucosa was significantly higher in mice co-treated with DSS and poly (I:C) than in those treated with poly (I:C) or DSS alone, suggesting that activation of pDCs was effectively induced in the colonic mucosa of mice treated with both DSS and poly (I:C). The number of $CD3^+$ T cells in the colonic mucosa was higher upon exposure to DSS in the presence or absence of poly (I:C)

treatment than that in untreated animals (Supplementary Fig. 1B and 1C). Consistent with the accumulation of pDCs in the colon, the expression levels of IFN-α and IL-33 in the colonic mucosa were markedly increased in mice treated with a combination of DSS and poly (I:C) as compared with their levels in the colonic mucosa in other three groups of mice (Supplementary Fig. 1D). Thus, the colon and pancreas share pathogenic immune responses leading to the development of AIP in that activation of IFN-α- and IL-33-producing pDCs was effectively induced in both organs upon exposure to DSS and poly (I:C).

Combined treatment with DSS and poly (I:C) does not alter the accumulation of IFN-α- and IL-33-producing pDCs in the salivary glands

Having confirmed that combined treatment with DSS and poly (I:C) enhanced the activation of pDCs not only in the pancreas but also in the colon, we next addressed whether such treatment also affects the degree of accumulation of pDCs in the salivary glands. As shown in Supplementary Fig. 2A and 2C, repeated injections of poly (I:C) induced the accumulation of pDCs into the salivary glands, which was not enhanced by the combined treatment with DSS. DSS treatment alone did not induce the accumulation of pDCs in the salivary glands, but reduced the percentage of $CD3^+$ T cells in the salivary glands (Supplementary Fig. 2B and 2C). Consistent with the increased percentage of pDCs in the salivary glands of poly (I:C)-treated mice with or without exposure to DSS, poly (I:C) treatment alone was sufficient for the production of IFN-α and IL-33 in the salivary glands (Supplementary Fig. 2D). Thus, the percentages of IFN-α- and IL-33-producing pDCs were comparable in mice treated with poly (I:C) alone and in those treated with both poly (I:C) and DSS. These findings partially explain the lack of

significant differences in the severity of autoimmune sialadenitis in mice treated with poly (I:C) and DSS compared to that in animals treated with poly (I:C) alone. Taken together, these data suggest that the intestinal barrier dysfunction exacerbates AIP, but not autoimmune sialadenitis, through the activation of IFN-α- and IL-33-expressing pDCs.

Combined treatment with DSS and poly (I:C) exacerbates AIP through the activation of IFN-α-and IL-33-producing pDCs

We next addressed whether exacerbation of AIP by combined treatment with DSS and poly (I:C) depends upon activation of pDCs producing IFN-α and IL-33. To this end, mice co-treated with DSS and poly (I:C) received IP injections of 120G8 Ab to deplete pDCs. As shown in Fig. 3A, treatment with 120G8 Ab led to a significant reduction in the percentages of pancreatic pDCs as compared with control Ab. The severity of AIP was smaller in mice treated with 120G8 Ab than in those with control Ab in pathological examinations (Fig. 3B). Furthermore, the depletion of pDCs reduced pancreatic expression of IFN-α and IL-33 (Fig. 3C). Neutralization of IFN-α-mediated signaling pathways by anti-IFNAR Ab also prevented the exacerbation of AIP induced by combined treatment with DSS and poly (I:C) (data not shown). Thus, these data suggest that pDCs producing IFN-α and IL-33 mediate exacerbation of AIP induced by co-treatment with DSS and poly (I:C).

The depletion of pDCs by 120G8Ab did not completely protect mice from AIP induced by DSS and poly (I:C). This is probably because the depletion efficiency by 120G8Ab was approximately 50% in this study. Alternatively, IL-33 produced by non-

hematopoietic cells (pancreatic acinar cells) might promote chronic fibroinflammatory responses characterizing AIP through activation of group 2 innate lymphoid cells (9,32).

Exacerbation of AIP is associated with increased translocation of intestinal bacteria into the pancreas

Having found that immune responses associated with the development of AIP are shared in the pancreas and colon, we next tried to determine whether intestinal dysbiosis followed by pancreatic translocation of bacteria may play a pathogenic role in the development of severe AIP caused by intestinal barrier dysfunction. For this purpose, we performed 16S rRNA sequencing of stool and pancreatic samples as described previously (6,10). As shown in Supplementary Fig. 3A, equivalent numbers of sequence reads were obtained in both fecal and pancreatic samples in all the four groups. Fecal samples obtained from mice treated with DSS exhibited reduced microbial diversity according to the rarefaction analysis of alpha diversity (Supplementary Fig. 3B). Moreover, fecal samples exhibited treatment-specific microbial composition community upon visualization of beta diversity in three-dimensional scatter plot by PCoA (Supplementary Fig. 3C). In contrast, microbial diversity was comparable in the pancreas of the four groups of mice in both the rarefaction analysis of alpha diversity and PCoA of beta diversity. Thus, the disruption of the intestinal barrier by DSS in combination with poly (I:C) did not alter pancreatic microbial diversity.

We semi-quantitatively measured bacterial amounts in the pancreas. DNA extracted from the pancreas was subjected to quantitative PCR analyses using primers for 16S rRNA V3-V4 regions. Results were shown as relative amounts of pancreatic bacterial DNA to those

in the ileum as a reference. As shown in Supplementary Fig. 4A, relative amounts of pancreatic DNA were significantly higher in mice treated with DSS and poly (I:C) compared with the other groups.

Exacerbation of AIP is associated with translocation of **Staphylococcus sciuri** *into the pancreas*

Next, we performed differential abundance analyses to identify bacterial species associated with the exacerbation of AIP in mice treated with both DSS and poly (I:C). For this purpose, we employed the R package ALDEx2 (27,28). However, we could not identify specific bacterial species in the pancreas as judged by *P* value or effect size in ALDEx2. Unidentified *Pseudomonas* species corresponded to more than 50% of the bacteria detected in the pancreas, although no difference was seen in the fraction of these bacteria in the four groups of mice (Supplementary Fig. 4B and 5). Unidentified members of the family *Enterobacteriaceae* were also abundant and corresponded to 10% of the bacteria detected in the pancreas in all four groups. *Staphylococcus sciuri* was detected in the pancreas of mice treated with DSS and poly (I:C) (Supplementary Fig. 4B and 5). In contrast, this bacterium was not detected in any of the other three groups of mice. Similarly, unidentified *Dorea* species, *Akkermansia muciniphila*, and unidentified *Odoribacter* species were preferentially detected in the pancreas of mice treated with DSS and poly (I:C), but not in the other three groups of mice (Supplementary Fig. 5). Thus, some unique bacteria, including *S. sciuri*, were detected in the pancreas of mice treated with DSS and poly (I:C) although they were not statistically significant.

ALDEx2 identified unidentified *Lactobacillus* species as significantly increased bacterial species in the stool of mice treated with DSS and poly (I:C) (Supplementary Fig. 6). The percentage of unidentified members of the family S24-7 was decreased in the stools of mice treated with DSS and poly (I:C) as compared with that in the other three groups (Supplementary Fig. 6). However, neither of these bacteria was preferentially detected in the pancreas of mice treated with DSS and poly (I:C). The percentage of *Akkermansia muciniphila* was decreased in the stools of mice treated with DSS and/or poly (I:C). Unknown *Turicibacter* species were decreased in the stools of mice treated with DSS and poly (I:C) or in those treated with poly (I:C) alone, whereas the colonization of the pancreas by this bacterium was comparable between mice treated with DSS alone and those treated with DSS and poly (I:C). Moreover, unidentified *Pseudomonas* species, which were abundant in the pancreas, were not detected in the stool of any groups of mice. Among the bacteria preferentially detected in the pancreas of mice treated with DSS and poly (I:C), *S. sciuri* was the only bacterium that was found in more than 50% of the mice. In addition, the degree of AIP was much more severe in mice exhibiting pancreatic colonization by *S. sciuri* than in those without it (data not shown). 16S rRNA sequencing of stool and pancreatic samples suggested that exacerbation of AIP by the disruption of the epithelial barrier might be caused by the translocation of *S. sciuri* from the gut to the pancreas. Based on this assumption, we next performed experiments focusing on immune responses against *S. sciuri.*

***Pancreatic pDCs isolated from mice co-treated with poly (I:C) and DSS produce large amount of IFN-a and IL-33 upon exposure to* S. sciuri**

Translocation of *S. sciuri* from the gut to the pancreas might alter sensitivity of pDCs to this bacterium and thus modulate production of IFN-α and IL-33. To examine this issue, pancreatic pDCs isolated from mice treated with poly (I:C) and/or DSS were stimulated with various kinds of gut bacteria including *S. sciuri in vitro* (Fig. 4). Consistent with our previous reports (6,10), pancreatic pDCs produced much greater amounts of IFN-α and IL-33 upon stimulation with *K. pneumoniae* as compared with *B. pseudolongum*. Pancreatic pDCs produced comparable levels of these cytokines whether mice were treated with poly (I:C) alone or with both poly (I:C) and DSS *in vivo*. Thus, pancreatic pDCs isolated from poly (I:C)-treated mice produced large amounts of IFN-α and IL-33 upon exposure to *K. pneumoniae* in the presence or absence of intestinal barrier dysfunction. Production of IFN-α and IL-33 was smaller in pancreatic pDCs from mice treated with poly (I:C) alone upon *in vitro* stimulation with *S. sciuri* as compared with *K. pneumoiae*. It should be noted, however, that production of IFN-α and IL-33 by pDCs from mice treated with both poly (I:C) and DSS was comparable whether these cells were stimulated with *S, sciuri* or *K. pneumoniae*. Thus, *in vitro* exposure to *S. sciuri* markedly enhanced production of IFN-α and IL-33 by pDCs from mice treated with both DSS and poly (I:C) compared with those from mice treated with poly (I:C) alone.

S. aureus often colonize in the GI tract and cause bloodstream infections (33). Although we have not confirmed colonization of this bacterium in the pancreas or stool in mice treated with both DSS and poly (I:C), we tried to verify whether augmentation of IFN-α and IL-33 was specific to *S. sciuri*, but not *S. aureus*. As shown in Supplementary Fig. 7, production of IFN-α and IL-33 by pancreatic pDCs upon *in vitro* exposure to *S. aureus* was comparable whether mice were treated with poly (I:C) alone or with both poly (I:C)

and DSS. Thus, combined treatment with poly (I:C) and DSS increased sensitivity of pDCs to *S, sciuri,* but not *K. pneumoniae* or *S. aureus*, in terms of pathogenic cytokine production, as compared with poly (I:C) treatment alone. Collectively, these *in vitro* experiments suggest that translocation of *S. sciuri* from the gut into the pancreas increased sensitivity of pDCs to this bacterium to produce large amount of IFN-α and IL-33.

GF mice mono-colonized with* S. sciuri *develop severe experimental AIP upon treatment with low doses of poly (I:C)

The link between the exacerbation of experimental AIP, pancreatic translocation of *S. sciuri*, and enhanced sensitivity of pDCs to this bacterium prompted us to examine the pathogenicity of this bacterium. For this purpose, we utilized GF MRL/MpJ mice mono-colonized with *S. sciuri* that were treated with low doses (10 μg) of poly (I:C) or left untreated (control group). As was shown in our previous studies (6,10), repeated injections of 10 μg of poly (I:C) resulted in mild experimental AIP. Therefore, we hypothesized that GF mice mono-colonized with *S. sciuri* would develop moderate or severe experimental AIP upon treatment with 10 μg of poly (I:C) if this bacterium had the ability to promote chronic pancreatic inflammation.

In accordance with our previous observations, repeated injections of 10 μg of poly (I:C) induced mild experimental AIP in GF mice (Fig. 5A). However, GF mice mono-colonized with *S. sciuri* developed severe pancreatitis upon exposure to the same dose of poly (I:C). It should be noted that GF mice mono-colonized with *S. sciuri* did not develop AIP spontaneously without poly (I:C) treatment (Fig. 5A). In contrast, the degree of autoimmune sialadenitis upon exposure to repeated injections of 10 μg of poly (I:C) was

comparable between naive GF mice and GF mice mono-colonized with *S. sciuri* (Fig. 5A). Colitis was not observed in any group of mice (data not shown). Semi-quantitative assessment of AIP by scoring also confirmed that the degree of AIP was much greater in GF mice mono-colonized with *S. sciuri* than in non-colonized GF mice upon treatment with 10 μg of poly (I:C) (Fig. 5B). No significant difference was observed in the pathological scores of poly (I:C)-induced autoimmune sialadenitis between non-colonized GF mice and GF mice mono-colonized with *S. sciuri*. Thus, GF mice mono-colonized with *S. sciuri* developed severe AIP upon treatment with 10 μg of poly (I:C), a dose that usually causes mild AIP. Therefore, the results obtained from GF mice and GF mice mono-colonized with *S. sciuri* strongly suggest that colonization by *S. sciuri* plays a pathogenic role in the development of AIP.

IFN-α- and IL-33-producing pDCs mediate severe AIP in GF mice mono-colonized with* S. sciuri *and treated with low doses of poly (I:C)

In the final series of experiments, we examined whether the development of severe AIP in GF mice mono-colonized with *S. sciuri* and treated with poly (I:C) was associated with pancreatic accumulation of IFN-α- and IL-33-producing pDCs. As shown in Fig. 6A, the percentage of pDCs was much greater in the pancreas of GF mice mono-colonized with *S. sciur*i and treated with poly (I:C) than in GF mice that received either of these two treatments alone. In contrast, no significant difference was observed between these groups of mice in the percentage of pDCs in the salivary glands. Thus, these flow-cytometry analyses strongly suggest that pDCs accumulated in the pancreas of GF mice mono-colonized with *S. sciuri* and treated with poly (I:C).

Consistent with the enhanced pancreatic accumulation of pDCs in GF mice mono-colonized with *S. sciuri* and treated with poly (I:C), the expression levels of IFN-α and IL-33 were also much greater in the pancreas of these animals than in GF mice only mono-colonized with *S. sciuri* or in those treated only with poly (I:C) (Fig. 6B). Thus, colonization with *S. sciuri* and treatment with poly (I:C) enhanced the pancreatic expression levels of IFN-α and IL-33 as compared to those in other groups of mice. In contrast, no significant difference was observed in the expression levels of IFN-α or IL-33 in the salivary glands of poly (I:C)-treated GF mice with or without colonization of *S. sciuri*. Colonization by *S. sciuri* in combination with repeated injections of 10 μg of poly (I:C) promoted pancreatic accumulation of pDCs and induced the expression of IFN-α and IL-33 in the pancreas of GF mice, thereby causing severe AIP. Taken together, these data suggest that colonization with *S. sciuri* exacerbated experimental AIP, but not autoimmune sialadenitis, through the activation of IFN-α- and IL-33-producing pDCs.

Discussion

AIP and IgG4-RD are characterized not only by enhanced IgG4 Ab responses but also by multiple organ injury (1-4). These autoimmune disorders preferentially occur in the pancreas, salivary glands, kidneys, lungs, and bile ducts (1-4). Although multiple organs are damaged simultaneously and metachronously in patients with AIP and IgG4-RD, the molecular mechanisms accounting for the development of pancreatic and extra-pancreatic inflammation are poorly understood. Given that the disruption of the intestinal barrier associated with leaky gut plays a pathogenic role in the development of extra-GI autoimmune diseases (14,15,34), it is likely that intestinal barrier dysfunction underlies the immunopathogenesis of multiple organ involvement in AIP and IgG4-RD. In this study, we explored the roles played by intestinal dysbiosis in the development of pancreatic and extra-pancreatic manifestations associated with AIP and IgG4-RD. To this end, we utilized a well-established experimental AIP and autoimmune sialadenitis model, MRL/MpJ mice treated with repeated injections of poly (I:C) (16), in combination with the disruption of the intestinal barrier by exposure to DSS (17,18). Here, we provide evidence that intestinal barrier dysfunction exacerbates AIP, but not autoimmune sialadenitis, through the translocation of *S. sciuri* into the pancreas and activation of IFN-α- and IL-33-producing pDCs. This conclusion was supported by the following findings presented in this manuscript. First, the severity of AIP was greater in mice co-treated with DSS and poly (I:C) than in those treated with poly (I:C) alone. In contrast, the severity of autoimmune sialadenitis was comparable between these two groups. Second, the percentage of IFN-α- and IL-33-producing pDCs was greater in the pancreas of mice co-treated with DSS and poly (I:C) than that in mice treated with poly (I:C) alone, whereas no significant difference was observed in the percentage of pDCs in the salivary glands.

In addition, the depletion of pDCs by 120G8 Ab prevented exacerbation of AIP induced by co-treatment with DSS and poly (I:C). Third, 16S rRNA sequencing revealed that the translocation of *S. sciuri* into the pancreas from the GI tract was observed in mice co-treated with poly (I:C) and DSS. Fourth, pancreatic pDCs isolated from mice treated with both poly (I:C) and DSS, but not poly (I:C) alone, exhibited increased sensitivity to *S. sciuri* to produce large amounts of IFN-α and IL-33. Fifth, gnotobiotic mice with *S. sciuri* developed severe AIP, but not autoimmune sialadenitis, upon repeated injections of a low dose of poly (I:C), which usually induces mild AIP (6,10). Interestingly, the development of severe AIP in gnotobiotic mice with *S. sciuri* was accompanied by pancreatic accumulation of IFN-α- and IL-33-producing pDCs. Taken together, these data suggest that intestinal barrier dysfunction exacerbated AIP through the pancreatic translocation of *S. sciuri* and accumulation of pDCs.

It has been established that low-grade inflammation in older adults is sometimes associated with increased intestinal epithelial permeability and intestinal dysbiosis (11-13). The typical patients with AIP and IgG4-RD are middle-aged to elderly men (1-4). This epidemiological feature led us to speculate that intestinal barrier dysfunction is involved in the immunopathogenesis of AIP and IgG4-RD. Although we previously reported the involvement of intestinal dysbiosis in the development of experimental and human AIP (6,10), the role of the intestinal barrier dysfunction has been poorly defined. In this study, we found that the disruption of the intestinal barrier by DSS exacerbated AIP induced by repeated injections of poly (I:C), which was accompanied by pancreatic accumulation of IFN-α- and IL-33-producing pDCs. Our 16S rRNA sequencing studies revealed predominant colonization of unidentified *Pseudomonas* species in the pancreas

of mice treated with or without DSS or poly (I:C), suggesting contamination by environmental bacteria during the preparation of pancreatic samples. However, treatment with a combination of poly (I:C) and DSS promoted translocation of intestinal bacteria into the pancreas as shown by our findings that amounts of bacterial DNA were much greater in mice treated with both DSS and poly (I:C) than in those with the other groups. Thus, disruption of intestinal barrier by DSS acts together with induction of AIP by poly (I:C) to promote translocation of intestinal bacteria into the pancreas. In addition, treatment with a combination of poly (I:C) and DSS led to the accumulation of pDCs and enhanced production of IFN-α and IL-33 not only in the colonic mucosa, but also in the pancreas of MRL/MpJ mice, suggesting the presence of the gut-pancreas axis that mediated the exacerbation of AIP. In contrast, the gut-salivary gland axis was not involved, because no significant differences were seen in the percentage of pDCs or in the production of IFN-α or IL-33 in the salivary glands of mice co-treated with poly (I:C) and DSS and those treated with poly (I:C) alone. Moreover, intestinal barrier dysfunction followed by the translocation of *S. sciuri* into the pancreas promoted the development of chronic fibroinflammatory responses, as was shown by observations in GF mice mono-colonized with *S. sciuri* and treated with low doses (10 μg) of poly (I:C). In these animals, pancreatic accumulation of IFN-α- and IL-33-producing pDCs was markedly increased, as in mice treated with both DSS and poly (I:C). Thus, the disruption of the intestinal barrier aggravated AIP through the pancreatic translocation of *S. sciuri* and activation of pDCs. Consistent with this idea, Sorini et al. reported that a loss of the gut barrier integrity contributes to the development of autoimmune diabetes (35). Thus, our study, together with previous reports, supports the notion that intestinal barrier dysfunction, intestinal dysbiosis, and bacterial translocation might be important pathogenic factors for the

development of AIP and IgG4-RD in the elderly. Verification of this idea requires further studies addressing gut barrier integrity in patients with AIP and IgG4-RD.

S. sciuri is a gram-positive, oxidase-positive, coagulase-negative member of the bacterial genus *Staphylococcus* (36-38). This bacterium has been isolated from the skin and stools of mammals, including humans (39,40). Interestingly, the development of severe AIP seen in mice treated with a combination of poly (I:C) and DSS was accompanied by the translocation of *S. sciuri* into the pancreas. Moreover, GF mice developed severe AIP upon colonization by *S. sciuri* and treatment with low doses of poly (I:C), which normally causes mild AIP on its own. These data strongly suggest that *S. sciuri* exerts a pathogenic effect on the development of experimental AIP. It should be noted that pancreatic colonization by *S. sciuri* alone is not sufficient to trigger experimental AIP because GF mice mono-colonized with this bacterium did not develop AIP unless they were injected with low doses of poly (I:C). Therefore, the role of *S. sciuri* is likely to intensify pancreatic inflammation rather than to actually cause it. As for the molecular mechanisms of how pancreatic colonization by *S. sciuri* promotes the development of experimental AIP, Hagner et al. reported that intranasal administration of *S. sciuri* prevented the development of house dust mite extract-induced airway inflammation caused by Th2 responses (41). Stimulation of human monocyte-derived dendritic cells with *S. sciuri* upregulated the expression of co-stimulatory molecules and Th1-related cytokines (IL-12p35, IL-12p40, IL-23p19) through the activation of Toll-like receptor 2 (TLR2) and nucleotide-binding oligomerization domain 2 (NOD2) (41,42). Therefore, it is possible that colonization by *S. sciuri* promoted chronic fibroinflammatory responses in the pancreas through the activation of TLR2 and NOD2 in pDCs followed by Th1 responses.

Consistent with this idea, pDCs have been reported to express functional NOD2 (43). Infection with this bacterium has been reported to cause peritonitis, sepsis, and endocarditis (37,38,44). In addition to these infectious diseases, our data highlight the importance of *S. sciuri* in the development of AIP and IgG4-RD. However, we have to be cautious regarding the interpretation of the pathogenicity of *S. sciuri* in the development of human AIP and IgG4-RD, given that we failed to identify this bacterium in the feces of three patients with these disorders (data not shown). Future studies proving the presence of *S. sciuri* in the stools of a large number of patients with AIP and IgG4-RD are required to establish the link between colonization with this bacterium and disease development. Moreover, we have not confirmed the virulence of *S. sciuri* isolated from the stool of MRL/MpJ mice treated with both DSS and poly (I:C) because we used a commercially available bacterial strain. Although the virulence of commercially available *S. sciuri* has been confirmed in gnotobiotic and *in vitro* experiments, such experiments employing *S. sciuri* isolated from the stool might be required to determine the pathogenicity of this bacterium.

Regarding the ability of *S. sciuri* to induce activation of pDCs, gnotobiotic mice with *S. sciuri* displayed enhanced accumulation of pancreatic pDCs producing IFN-α upon repeated injections of low doses of poly (I:C). Although GF mice have been shown to bear developmental defects in immune systems (45,46), comparable levels of percentages of pancreatic pDCs (5-10%) and enhanced levels of pancreatic IFN-α production (15-20 vs. 5-10 pg/mg) were observed in our GF MRL/MpJ mice upon treatment with low doses of poly (I:C) as compared with specific pathogen free MRL/MpJ mice with the same poly (I:C) treatment (6,10). It should be noted that colonization of *S. sciuri* with GF mice

markedly increased pancreatic accumulation of pDCs (15-20%) and production of IFN-α (30-40 pg/mg) when these mice were treated with low doses of poly (I:C). Notably, repeated injections of low doses of poly (I:C) induced similar levels of activation of pancreatic pDCs (15-20%) and reduced levels in pancreatic IFN-α production (10-15 pg/mg) in MRL/MpJ mice that received fecal microbiota from mice displaying severe AIP compared with gnotobiotic mice with *S. sciuri* (6). Therefore, the results in this study together with our previous data support the view that *S. sciuri* functions as one of the pathogenic bacteria causing experimental AIP in terms of its ability to induce activation of pDCs. Verification of this view awaits the results of studies in which responses to low doses of poly (I:C) are examined in gnotobiotic MRL/MpJ mice with *S. sciuri* or with one of the major commensal bacteria such as *Bacteroides* or *Bifidobacterium* species.

We as well as other researchers have provided evidence that intestinal dysbiosis underlies the immunopathogenesis of AIP and IgG4-RD (6,47). In subsequent studies, we found that the disappearance of *K. pneumoniae* from the gut was associated with the induction of remission by prednisolone in two of three patients with AIP (10). The severity of AIP was greater in mice treated with repeated injections of low doses of poly (I:C) (10 μg), in combination with oral administration of heat-killed *K. pneumoniae* than in those treated with poly (I:C) or with *K. pneumoniae* alone (10). In addition, pDCs isolated from the pancreas of AIP mice produced large amounts of IFN-α and IL-33 upon stimulation with heat-killed *K. pneumoniae* (10). As in the case of colonization by *S. sciuri*, colonization by *K. pneumoniae* alone was not sufficient for the development of experimental AIP (10). Thus, intestinal colonization by *K. pneumoniae* might play an important role in the development of AIP and IgG4-RD. However, no significant alterations in the proportions

of *K. pneumoniae* were observed in our 16S rRNA sequencing studies of fecal and pancreatic samples from mice treated with DSS and/or poly (I:C). Therefore, it is unlikely that immune responses against *K. pneumoniae* contributed to the exacerbation of experimental AIP triggered by intestinal barrier dysfunction. Consistent with this idea, pancreatic pDCs produced comparable levels of IFN-α and IL-33 upon stimulation with *K. pneumoniae* whether mice were treated with both poly (I:C) and DSS or poly (I:C) alone.

IFN-α- and IL-33-producing pDCs play pivotal roles in the development of experimental AIP, as has been shown in our previous studies in which the depletion of pDCs or the neutralization of IFN-α and IL-33 efficiently suppressed chronic fibroinflammatory responses in the pancreas of MRL/MpJ mice treated with repeated injections of poly (I:C) (5,9). In addition, IFN-α- and IL-33-producing pDCs were located in the pancreas of individuals with AIP and IgG4-RD (5,9), and the serum concentrations of both cytokines were identified as new biomarkers for these autoimmune disorders (8). Thus, enhanced production of IFN-α and IL-33 by pDCs underlies the immunopathogenesis of experimental AIP and human IgG4-associated AIP. In this study, repeated injections of high doses (100 μg) of poly (I:C) into MRL/MpJ mice led to accumulation of pDCs accompanied by increased production of IFN-α and IL-33 not only in the pancreas but also in the salivary glands. Thus, the pancreas and salivary glands share pathogenic immune responses leading to the development of chronic inflammation, in which pDCs producing IFN-α and IL-33 infiltrate into the tissues. Therefore, these data suggest that activation of pDCs might mediate both AIP and autoimmune sialadenitis as organ-specific manifestations of systemic IgG4-RD through the production of IFN-α and IL-33.

Furukawa et al. reported that M2 macrophages, but not pDCs, produce IL-33 in the salivary glands of patients with IgG4-RD (48,49). In contrast to the case of experimental AIP and autoimmune sialadenitis, cellular sources of IL-33 may be different in the pancreas and salivary glands of patients with IgG4-RD, suggesting that IL-33 may play pathogenic roles in IgG4-associated autoimmune sialadenitis, independent of pDC activation.

Intestinal barrier disruption exacerbated experimental AIP, but not autoimmune sialadenitis, in this study. Thus, intestinal barrier dysfunction is unlikely to play a pathogenic role in the development of autoimmune sialadenitis. Consistent with this idea, no significant alterations were observed in the percentage of IFN-α- and IL-33-producing pDCs in the salivary glands of mice treated with poly (I:C) alone and of those treated with poly (I:C) and DSS. In addition, GF mice mono-colonized with *S. sciuri* exhibited a similar degree of autoimmune sialadenitis to that observed in GF mice upon treatment with repeated injections of poly (I:C), which effects were parallel to the percentages of IFN-α- and IL-33-producing pDCs. The molecular mechanisms that precluded negative effects of intestinal barrier dysfunction on autoimmune sialadenitis are currently unknown. In this regard, we speculate that dysbiosis of the oral rather than gut microbiota might be involved in the development of autoimmune sialadenitis. In agreement with this notion, a link between oral dysbiosis and primary Sjogren's syndrome has been reported (50-52). Therefore, the disruption of oral barrier function followed by oral dysbiosis might be one of the possible triggers for the development of autoimmune sialadenitis associated with AIP and IgG4-RD. Confirmation of this hypothesis requires examination

of immune responses and bacterial translocation in the pancreas and salivary glands of patients with AIP and IgG4-RD.

In conclusion, we have elucidated several molecular mechanisms by which the gut-pancreas axis contributes to the development and exacerbation of AIP. Intestinal barrier dysfunction followed by intestinal dysbiosis underlies the immunopathogenesis of experimental AIP through the activation of IFN-α- and IL-33-producing pDCs. We identified *S. sciuri* as a candidate pathogenic bacterium using 16S rRNA sequencing of pancreatic and stool samples. *S. sciuri* pathogenicity was verified in experiments on gnotobiotic mice, in which GF mice mono-colonized with *S. sciuri* developed severe AIP through the activation of IFN-α- and IL-33-producing pDCs. Thus, patients with AIP and IgG4-RD may be efficiently treated by using therapies aimed at the restoration of the intestinal barrier function.

Acknowledgements

The authors would like to thank Ms. Yukiko Ueno for her secretarial assistance.

Funding

This work was supported by Grants-in-Aid for Scientific Research (21K15987, 22K08090, 22K07996) from the Japan Society for the Promotion of Science, Takeda Science Foundation, Yakult Bio-Science Foundation, SENSHIN Medical Research Foundation, 2022 Kindai University Research Enhancement Grant (KD2208) and Japan Agency for Medical Research and Development (AMED) for Research on Intractable Diseases.

Figure legends

Figure 1. Disruption of the intestinal barrier exacerbates autoimmune pancreatitis, but not autoimmune sialadenitis in MRL/MpJ mice. (A) Schedule of intraperitoneal injections of polyinosinic-polycytidylic acid (poly (I:C)) and/or administration of 2% dextran sodium sulfate (DSS) in the drinking water. Mice received intraperitoneal injections of poly (I:C) (100 μg) for a total of 15 times and/or 2% DSS in the drinking water every two weeks for a total of 7 weeks. Four groups of MRL/MpJ mice were used: mice without treatment (n = 7), mice treated with 2% DSS in the drinking water (n = 9), mice treated with poly (I:C) (n = 12), and mice treated with both DSS and poly (I:C) (n = 14). **(B)** Histopathological findings in the pancreas, colon, and salivary glands of MRL/MpJ mice treated with DSS and/or poly (I:C). Hematoxylin and eosin staining. Scale bar; 100 μm for the pancreas and salivary glands, 200 μm for the colon. **(C)** Pathological scores of autoimmune pancreatitis, colitis, and autoimmune sialadenitis were determined as described in Materials and Methods. Results are expressed as the mean $\pm$ SE. *$P < 0.05$, **$P < 0.01$, n.s. (not significant).

Figure 2. Accumulation of plasmacytoid dendritic cells in the pancreas of mice treated with a combination of dextran sodium sulfate and polyinosinic-polycytidylic acid. (A–C) Pancreatic accumulation of plasmacytoid dendritic cells (pDCs) in four groups of MRL/MpJ mice: mice without treatment (n = 5), mice treated with 2% dextran sodium sulfate (DSS) in the drinking water (n = 10), mice treated with polyinosinic-polycytidylic acid (poly (I:C)) (n = 11), and mice treated with both DSS and poly (I:C) (n = 12). Representative dot plots of flow-cytometry analyses are illustrated. Pancreatic immune cells were stained with FITC-conjugated anti-B220 Ab and PE-conjugated anti-PDCA-1 Ab. Cells were also stained with FITC-conjugated anti-B220 Ab and PE-conjugated anti-CD3 Ab. pDCs were defined as PDCA-1^+ $B220^{low}$ cells. The percentages and numbers of pDCs, $CD3^+$ T cells, and $B220^+$ B cells are shown. **(D)** Pancreatic expression of IFN-α and IL-33 measured by the enzyme-linked immunosorbent assay. Results are expressed as the mean ± SE. **P* < 0.05, ***P* < 0.01, n.s. (not significant).

Figure 3. Exacerbation of autoimmune pancreatitis induced by a combination of dextran sodium sulfate and polyinosinic-polycytidylic acid depends upon activation of plasmacytoid dendritic cells. MRL/MpJ mice received intraperitoneal injections of poly (I:C) (100 μg) for a total of 15 times and/or 2% dextran sodium sulfate (DSS) in the drinking water every two weeks for a total of 7 weeks. Mice also received intraperitoneal injections of 120G8 Ab (n = 7, 0.1 mg/each mouse) or control IgG Ab (n = 9, 0.1 mg) prior to each poly (I:C) injection. **(A)** Pancreatic accumulation of plasmacytoid dendritic cells (pDCs) is illustrated by representative dot plots of flow-cytometry analysis. Immune cells isolated from the pancreas were stained with FITC-conjugated anti-B220 Ab and PE-conjugated anti-PDCA-1 Ab. pDCs were defined as PDCA-1^+B220^{low} cells. The

percentage of pDCs is shown. **(B)** Histopathological findings in the pancreas of mice. Hematoxylin and eosin staining. Scale bar; 100 μm. Pathological scores of autoimmune pancreatitis were determined as described in Materials and Methods. Results are expressed as the mean ± SE. **(C)** Pancreatic expression of IFN-α and IL-33 measured by the enzyme-linked immunosorbent assay. $^{**}P < 0.01$.

Figure 4. Pancreatic plasmacytoid dendritic isolated from the mice treated with both dextran sodium sulfate and polyinosinic-polycytidylic acid exhibit increased sensitivity to *Staphylococcus sciuri*. Plasmacytoid dendritic cells (pDCs) were identified as PDCA-$1^{+}B220^{low}$ cells and FACS-sorted. pDCs ($5x10^{5}$/mL) were stimulated with *Bifidobacterium pseudolongum*, *Klebsiella pneumoniae*, and *Staphylococcus sciuri* at the indicated doses for 48 hrs. Cell culture supernatants were subjected to enzyme-linked immunosorbent assay to detect IFN-α and IL-33. **(A)** Gating strategy for isolation of pDCs. Immune cells isolated from the pancreas were stained with FITC-conjugated anti-B220, PerCP/Cy5.5-conjugated anti-CD3 Ab, APC-conjugated anti-PDCA-1 Ab. pDCs were defined as PDCA-$1^{+}B220^{low}$ cells. **(B)** Expression levels of IFN-α and IL-33 in the culture supernatants were measured. Results are expressed as the mean ± SE. $^{**}P < 0.01$, n.s. (not significant).

Figure 5. Development of severe autoimmune pancreatitis of germ-free mice mono-colonized with *Staphylococcus sciuri* upon treatment with low doses of polyinosinic-polycytidylic acid. Germ-free (GF) MRL/MpJ mice were untreated (n = 5) or treated with low doses (10 μg) of polyinosinic-polycytidylic acid (poly (I:C)) for a total of 16 times (n = 7). GF MRL/MpJ mice mono-colonized with *S. sciuri* were untreated (n = 6)

or treated with low doses of poly (I:C) for a total of 16 times (n = 7). **(A)** Histopathological findings in the pancreas and salivary glands of the four experimental groups of mice. Hematoxylin and eosin staining. Scale bar; 100 μm. **(B)** Pathological scores of autoimmune pancreatitis and autoimmune sialadenitis were determined as described in Materials and Methods. Results are expressed as the mean ± SE. *$P < 0.05$, **$P < 0.01$, n.s. (not significant).

Figure 6. Severe autoimmune pancreatitis of germ-free mice mono-colonized with *Staphylococcus sciuri* upon treatment with low doses of polyinosinic-polycytidylic acid is due to the pancreatic accumulation of IFN-α- and IL-33-producing plasmacytoid dendritic cells. Germ-free (GF) MRL/MpJ mice were untreated (n = 5) or treated with low doses (10 μg) of polyinosinic-polycytidylic acid (poly (I:C)) for a total of 16 times (n = 7). GF MRL/MpJ mice mono-colonized with *S. sciuri* were untreated (n = 6) or treated with low doses of poly (I:C) for a total of 16 times (n = 7). **(A)** Pancreatic accumulation of plasmacytoid dendritic cells (pDCs) is illustrated by representative dot plots of flow-cytometry analysis. Immune cells isolated from the pancreas and salivary glands were stained with FITC-conjugated anti-B220 Ab and PE-conjugated anti-PDCA-1 Ab. pDCs were defined as PDCA-1^{+}B220^{low} cells. The percentage of pDCs is shown. **(B)** Expression levels of IFN-α and IL-33 in the pancreas and salivary glands were measured by the enzyme-linked immunosorbent assay. Results are expressed as the mean ± SE. **$P < 0.01$, n.s. (not significant).

References

1 Stone, J. H., Zen, Y., and Deshpande, V. 2012. IgG4-related disease. *N Engl J Med* 366:539.

2 Kamisawa, T., Chari, S. T., Lerch, M. M., Kim, M. H., Gress, T. M., and Shimosegawa, T. 2013. Recent advances in autoimmune pancreatitis: type 1 and type 2. *Gut* 62:1373.

3 Kamisawa, T., Zen, Y., Pillai, S., and Stone, J. H. 2015. IgG4-related disease. *Lancet* 385:1460.

4 Watanabe, T., Minaga, K., Kamata, K., Kudo, M., and Strober, W. 2018. Mechanistic Insights into Autoimmune Pancreatitis and IgG4-Related Disease. *Trends Immunol* 39:874.

5 Arai, Y., Yamashita, K., Kuriyama, K., Shiokawa, M., Kodama, Y., Sakurai, T., Mizugishi, K., Uchida, K., Kadowaki, N., Takaori-Kondo, A., Kudo, M., Okazaki, K., Strober, W., Chiba, T., and Watanabe, T. 2015. Plasmacytoid Dendritic Cell Activation and IFN-alpha Production Are Prominent Features of Murine Autoimmune Pancreatitis and Human IgG4-Related Autoimmune Pancreatitis. *J Immunol* 195:3033.

6 Kamata, K., Watanabe, T., Minaga, K., Hara, A., Yoshikawa, T., Okamoto, A., Yamao, K., Takenaka, M., Park, A. M., and Kudo, M. 2019. Intestinal dysbiosis mediates experimental autoimmune pancreatitis via activation of plasmacytoid dendritic cells. *Int Immunol* 31:795.

7 Minaga, K., Watanabe, T., Arai, Y., Shiokawa, M., Hara, A., Yoshikawa, T., Kamata, K., Yamashita, K., and Kudo, M. 2020. Activation of interferon regulatory factor 7 in plasmacytoid dendritic cells promotes experimental autoimmune pancreatitis. *J Gastroenterol* 55:565.

8 Minaga, K., Watanabe, T., Hara, A., Kamata, K., Omoto, S., Nakai, A., Otsuka, Y., Sekai, I., Yoshikawa, T., Yamao, K., Takenaka, M., Chiba, Y., and Kudo, M. 2020. Identification of serum IFN-alpha and IL-33 as novel biomarkers for type 1 autoimmune pancreatitis and IgG4-related disease. *Sci Rep* 10:14879.

9 Watanabe, T., Yamashita, K., Arai, Y., Minaga, K., Kamata, K., Nagai, T., Komeda, Y., Takenaka, M., Hagiwara, S., Ida, H., Sakurai, T., Nishida, N., Strober, W., and Kudo, M. 2017. Chronic Fibro-Inflammatory Responses in Autoimmune Pancreatitis Depend on IFN-alpha and IL-33 Produced by Plasmacytoid Dendritic Cells. *J Immunol* 198:3886.

10 Kamata, K., Watanabe, T., Minaga, K., Hara, A., Sekai, I., Otsuka, Y., Yoshikawa, T., Park, A. M., and Kudo, M. 2020. Gut microbiome alterations in type 1

autoimmune pancreatitis after induction of remission by prednisolone. *Clin Exp Immunol* 202:308.

11 Ahmadi, S., Wang, S., Nagpal, R., Wang, B., Jain, S., Razazan, A., Mishra, S. P., Zhu, X., Wang, Z., Kavanagh, K., and Yadav, H. 2020. A human-origin probiotic cocktail ameliorates aging-related leaky gut and inflammation via modulating the microbiota/taurine/tight junction axis. *JCI Insight* 5.

12 Buford, T. W. 2017. (Dis)Trust your gut: the gut microbiome in age-related inflammation, health, and disease. *Microbiome* 5:80.

13 Kavanagh, K., Hsu, F. C., Davis, A. T., Kritchevsky, S. B., Rejeski, W. J., and Kim, S. 2019. Biomarkers of leaky gut are related to inflammation and reduced physical function in older adults with cardiometabolic disease and mobility limitations. *Geroscience* 41:923.

14 Mu, Q., Kirby, J., Reilly, C. M., and Luo, X. M. 2017. Leaky Gut As a Danger Signal for Autoimmune Diseases. *Front Immunol* 8:598.

15 Ilchmann-Diounou, H. and Menard, S. 2020. Psychological Stress, Intestinal Barrier Dysfunctions, and Autoimmune Disorders: An Overview. *Front Immunol* 11:1823.

16 Kamata, K., Watanabe, T., Minaga, K., Strober, W., and Kudo, M. 2018. Autoimmune Pancreatitis Mouse Model. *Curr Protoc Immunol* 120:15 31 1.

17 Watanabe, T., Asano, N., Murray, P. J., Ozato, K., Tailor, P., Fuss, I. J., Kitani, A., and Strober, W. 2008. Muramyl dipeptide activation of nucleotide-binding oligomerization domain 2 protects mice from experimental colitis. *J Clin Invest* 118:545.

18 Watanabe, T., Minaga, K., Kamata, K., Sakurai, T., Komeda, Y., Nagai, T., Kitani, A., Tajima, M., Fuss, I. J., Kudo, M., and Strober, W. 2019. RICK/RIP2 is a NOD2-independent nodal point of gut inflammation. *Int Immunol* 31:669.

19 Pfister, S. P., Scharen, O. P., Beldi, L., Printz, A., Notter, M. D., Mukherjee, M., Li, H., Limenitakis, J. P., Werren, J. P., Tandon, D., Cuenca, M., Hagemann, S., Uster, S. S., Terrazos, M. A., Gomez de Aguero, M., Schurch, C. M., Coelho, F. M., Curtiss, R., 3rd, Slack, E., Balmer, M. L., and Hapfelmeier, S. 2020. Uncoupling of invasive bacterial mucosal immunogenicity from pathogenicity. *Nat Commun* 11:1978.

20 Moltzau Anderson, J., Lipinski, S., Sommer, F., Pan, W. H., Boulard, O., Rehman, A., Falk-Paulsen, M., Stengel, S. T., Aden, K., Hasler, R., Bharti, R., Kunzel, S., Baines, J. F., Chamaillard, M., and Rosenstiel, P. 2020. NOD2 Influences

Trajectories of Intestinal Microbiota Recovery After Antibiotic Perturbation. *Cell Mol Gastroenterol Hepatol* 10:365.

21 Arvidsson, C., Hallen, A., and Backhed, F. 2012. Generating and Analyzing Germ-Free Mice. *Curr Protoc Mouse Biol* 2:307.

22 Qu, W. M., Miyazaki, T., Terada, M., Okada, K., Mori, S., Kanno, H., and Nose, M. 2002. A novel autoimmune pancreatitis model in MRL mice treated with polyinosinic:polycytidylic acid. *Clin Exp Immunol* 129:27.

23 Nishihara, M., Terada, M., Kamogawa, J., Ohashi, Y., Mori, S., Nakatsuru, S., Nakamura, Y., and Nose, M. 1999. Genetic basis of autoimmune sialadenitis in MRL/lpr lupus-prone mice: additive and hierarchical properties of polygenic inheritance. *Arthritis Rheum* 42:2616.

24 Watanabe, T., Sadakane, Y., Yagama, N., Sakurai, T., Ezoe, H., Kudo, M., Chiba, T., and Strober, W. 2016. Nucleotide-binding oligomerization domain 1 acts in concert with the cholecystokinin receptor agonist, cerulein, to induce IL-33-dependent chronic pancreatitis. *Mucosal Immunol* 9:1234.

25 Goodrich, J. K., Di Rienzi, S. C., Poole, A. C., Koren, O., Walters, W. A., Caporaso, J. G., Knight, R., and Ley, R. E. 2014. Conducting a microbiome study. *Cell* 158:250.

26 Okamoto, K., Watanabe, T., Komeda, Y., Okamoto, A., Minaga, K., Kamata, K., Yamao, K., Takenaka, M., Hagiwara, S., Sakurai, T., Tanaka, T., Sakamoto, H., Fujimoto, K., Nishida, N., and Kudo, M. 2018. Dysbiosis-Associated Polyposis of the Colon-Cap Polyposis. *Front Immunol* 9:918.

27 Rubin, I. M. C., Mollerup, S., Broholm, C., Knudsen, S. B., Baker, A., Helms, M., Holm, M. K. A., Kallemose, T., Westh, H., Dahl Knudsen, J., Pinholt, M., and Petersen, A. M. 2022. No Effect of Lactobacillus rhamnosus GG on Eradication of Colonization by Vancomycin-Resistant Enterococcus faecium or Microbiome Diversity in Hospitalized Adult Patients. *Microbiol Spectr*:e0234821.

28 Nearing, J. T., Douglas, G. M., Hayes, M. G., MacDonald, J., Desai, D. K., Allward, N., Jones, C. M. A., Wright, R. J., Dhanani, A. S., Comeau, A. M., and Langille, M. G. I. 2022. Microbiome differential abundance methods produce different results across 38 datasets. *Nat Commun* 13:342.

29 Chopyk, D. M. and Grakoui, A. 2020. Contribution of the Intestinal Microbiome and Gut Barrier to Hepatic Disorders. *Gastroenterology* 159:849.

30 Wells, J. M., Brummer, R. J., Derrien, M., MacDonald, T. T., Troost, F., Cani, P. D., Theodorou, V., Dekker, J., Meheust, A., de Vos, W. M., Mercenier, A., Nauta,

A., and Garcia-Rodenas, C. L. 2017. Homeostasis of the gut barrier and potential biomarkers. *Am J Physiol Gastrointest Liver Physiol* 312:G171.

31 Kiesler, P., Fuss, I. J., and Strober, W. 2015. Experimental Models of Inflammatory Bowel Diseases. *Cell Mol Gastroenterol Hepatol* 1:154.

32 Kiniwa, T. and Moro, K. 2021. Localization and site-specific cell-cell interactions of group 2 innate lymphoid cells. *Int Immunol* 33:251.

33 Kwiecinski, J. M. and Horswill, A. R. 2020. Staphylococcus aureus bloodstream infections: pathogenesis and regulatory mechanisms. *Curr Opin Microbiol* 53:51.

34 Fasano, A. 2012. Leaky gut and autoimmune diseases. *Clin Rev Allergy Immunol* 42:71.

35 Sorini, C., Cosorich, I., Lo Conte, M., De Giorgi, L., Facciotti, F., Luciano, R., Rocchi, M., Ferrarese, R., Sanvito, F., Canducci, F., and Falcone, M. 2019. Loss of gut barrier integrity triggers activation of islet-reactive T cells and autoimmune diabetes. *Proc Natl Acad Sci U S A* 116:15140.

36 Stepanovic, S., Vukovicc, D., Trajkovic, V., Samardzic, T., Cupic, M., and Svabic-Vlahovic, M. 2001. Possible virulence factors of Staphylococcus sciuri. *FEMS Microbiol Lett* 199:47.

37 Wallet, F., Stuit, L., Boulanger, E., Roussel-Delvallez, M., Dequiedt, P., and Courcol, R. J. 2000. Peritonitis due to Staphylococcus sciuri in a patient on continuous ambulatory peritoneal dialysis. *Scand J Infect Dis* 32:697.

38 Horii, T., Suzuki, Y., Kimura, T., Kanno, T., and Maekawa, M. 2001. Intravenous catheter-related septic shock caused by Staphylococcus sciuri and Escherichia vulneris. *Scand J Infect Dis* 33:930.

39 Couto, I., Sanches, I. S., Sa-Leao, R., and de Lencastre, H. 2000. Molecular characterization of Staphylococcus sciuri strains isolated from humans. *J Clin Microbiol* 38:1136.

40 Kmet, V., Cuvalova, A., and Stanko, M. 2018. Small mammals as sentinels of antimicrobial-resistant staphylococci. *Folia Microbiol (Praha)* 63:665.

41 Hagner, S., Harb, H., Zhao, M., Stein, K., Holst, O., Ege, M. J., Mayer, M., Matthes, J., Bauer, J., von Mutius, E., Renz, H., Heine, H., Pfefferle, P. I., and Garn, H. 2013. Farm-derived Gram-positive bacterium Staphylococcus sciuri W620 prevents asthma phenotype in HDM- and OVA-exposed mice. *Allergy* 68:322.

42 Kim, D., Kim, Y. G., Seo, S. U., Kim, D. J., Kamada, N., Prescott, D., Chamaillard, M., Philpott, D. J., Rosenstiel, P., Inohara, N., and Nunez, G. 2016. Nod2-

mediated recognition of the microbiota is critical for mucosal adjuvant activity of cholera toxin. *Nat Med* 22:524.

43 Castellaneta, A., Sumpter, T. L., Chen, L., Tokita, D., and Thomson, A. W. 2009. NOD2 ligation subverts IFN-alpha production by liver plasmacytoid dendritic cells and inhibits their T cell allostimulatory activity via B7-H1 up-regulation. *J Immunol* 183:6922.

44 Hedin, G. and Widerstrom, M. 1998. Endocarditis due to Staphylococcus sciuri. *Eur J Clin Microbiol Infect Dis* 17:673.

45 Kennedy, E. A., King, K. Y., and Baldridge, M. T. 2018. Mouse Microbiota Models: Comparing Germ-Free Mice and Antibiotics Treatment as Tools for Modifying Gut Bacteria. *Front Physiol* 9:1534.

46 Zheng, D., Liwinski, T., and Elinav, E. 2020. Interaction between microbiota and immunity in health and disease. *Cell Res* 30:492.

47 Hamada, S., Masamune, A., Nabeshima, T., and Shimosegawa, T. 2018. Differences in Gut Microbiota Profiles between Autoimmune Pancreatitis and Chronic Pancreatitis. *Tohoku J Exp Med* 244:113.

48 Furukawa, S., Moriyama, M., Miyake, K., Nakashima, H., Tanaka, A., Maehara, T., Iizuka-Koga, M., Tsuboi, H., Hayashida, J. N., Ishiguro, N., Yamauchi, M., Sumida, T., and Nakamura, S. 2017. Interleukin-33 produced by M2 macrophages and other immune cells contributes to Th2 immune reaction of IgG4-related disease. *Sci Rep* 7:42413.

49 Furukawa, S., Moriyama, M., Tanaka, A., Maehara, T., Tsuboi, H., Iizuka, M., Hayashida, J. N., Ohta, M., Saeki, T., Notohara, K., Sumida, T., and Nakamura, S. 2015. Preferential M2 macrophages contribute to fibrosis in IgG4-related dacryoadenitis and sialoadenitis, so-called Mikulicz's disease. *Clin Immunol* 156:9.

50 Alam, J., Lee, A., Lee, J., Kwon, D. I., Park, H. K., Park, J. H., Jeon, S., Baek, K., Lee, J., Park, S. H., and Choi, Y. 2020. Dysbiotic oral microbiota and infected salivary glands in Sjogren's syndrome. *PLoS One* 15:e0230667.

51 Lee, J., Alam, J., Choi, E., Ko, Y. K., Lee, A., and Choi, Y. 2020. Association of a dysbiotic oral microbiota with the development of focal lymphocytic sialadenitis in IkappaB-zeta-deficient mice. *NPJ Biofilms Microbiomes* 6:49.

52 van der Meulen, T. A., Harmsen, H. J. M., Vila, A. V., Kurilshikov, A., Liefers, S. C., Zhernakova, A., Fu, J., Wijmenga, C., Weersma, R. K., de Leeuw, K., Bootsma, H., Spijkervet, F. K. L., Vissink, A., and Kroese, F. G. M. 2019. Shared

gut, but distinct oral microbiota composition in primary Sjogren's syndrome and systemic lupus erythematosus. *J Autoimmun* 97:77.

Supplementary Figure 1. Accumulation of plasmacytoid dendritic cells in the colonic mucosa of mice treated with a combination of dextran sodium sulfate and polyinosinic-polycytidylic acid. (A–C) Colonic accumulation of plasmacytoid dendritic cells (pDCs) in four groups of mice: mice without treatment (n = 3), mice treated with 2% dextran sodium sulfate (DSS) in the drinking water (n = 4), mice treated with polyinosinic-polycytidylic acid (poly (I:C)) (n = 5), and mice treated with both DSS and poly (I:C) (n = 6). Representative dot plots of flow-cytometry analyses are illustrated. Colonic immune cells stained with FITC-conjugated anti-B220 Ab and PE-conjugated anti-PDCA-1 Ab. Cells were also stained with FITC-conjugated anti-B220 Ab and PE-conjugated anti-CD3 Ab. pDCs were defined as PDCA-1^{+} $B220^{low}$ cells. The percentages and numbers of pDCs, $CD3^{+}$ T cells, and $B220^{+}$ B cells are shown. **(D)** Colonic expression of IFN-α and IL-33 measured by the enzyme-linked immunosorbent assay. Results are expressed as the mean ± SE. $^{**}P < 0.01$, n.s. (not significant).

Supplementary Figure 2. Accumulation of plasmacytoid dendritic cells in the salivary glands of mice treated with a combination of dextran sodium sulfate and polyinosinic-polycytidylic acid. (A–C) Accumulation of plasmacytoid dendritic cells (pDCs) in the salivary glands in four groups of MRL/MpJ mice: mice without treatment (n = 3), mice treated with 2% dextran sodium sulfate (DSS) in the drinking water (n = 4), mice treated with polyinosinic-polycytidylic acid (poly (I:C)) (n = 5), and mice treated with both DSS and poly (I:C) (n = 6). Representative dot plots of flow-cytometry analyses are shown. Immune cells of the salivary glands were stained with FITC-conjugated anti-B220 Ab and PE-conjugated anti-PDCA-1 Ab. Cells were also stained with FITC-conjugated anti-B220 Ab and PE-conjugated anti-CD3 Ab. pDCs were defined as PDCA-

$1^{+}B220^{low}$ cells. The percentages and numbers of pDCs, $CD3^{+}$ T cells, and $B220^{+}$ B cells are shown. **(D)** Salivary gland expression of IFN-α and IL-33 measured by the enzyme-linked immunosorbent assay. Results are expressed as the mean ± SE. n.s. (not significant).

Supplementary Figure 3. Diversity of intestinal microbiota in the pancreas and stool of MRL/MpJ mice treated with polyinosinic-polycytidylic acid and/or dextran sodium sulfate. Stool and pancreas samples were subjected to 16S ribosomal RNA sequencing to evaluate the composition of intestinal microbiota in four groups of mice: mice without treatment (n = 3), mice treated with 2% dextran sodium sulfate (DSS) in the drinking water (n = 4), mice treated with polyinosinic-polycytidylic acid (poly (I:C)) (n = 5), and mice treated with both DSS and poly (I:C) (n = 6). **(A)** Number of sequence reads. **(B)** Rare faction analysis of alpha diversity in the stool and pancreas samples. **(C)** Differences in beta diversity were visualized in three-dimensional plots obtained from Principal-coordinate analysis.

Supplementary Figure 4. Relative amounts of bacterial DNA in the pancreas and stool of MRL/MpJ mice treated with polyinosinic-polycytidylic acid and/or dextran sodium. (A) DNA isolated from the stool and pancreas samples were subjected to quantitative PCR analyses targeting 16S ribosomal RNA to determine the relative amounts of bacterial DNA (n = 5 in each group). Bacterial DNA amounts in the ileum of non-treated MRL/MPJ mice were used as the reference. Four groups of mice were included: mice without treatment, mice treated with 2% dextran sodium sulfate (DSS) in the drinking water, mice treated with polyinosinic-polycytidylic acid (poly (I:C)), and

mice treated with both DSS and poly (I:C). *P < 0.05, **P < 0.01, n.s. (not significant). **(B)** The relative abundance of bacteria in the pancreas and stool is shown at the species level. Results are expressed as mean ± SE.

Supplementary Figure 5. Compositional alterations of intestinal microbiota in the pancreas of mice treated with polyinosinic-polycytidylic acid and/or dextran sodium sulfate. Pancreatic samples were subjected to 16S ribosomal RNA sequencing to evaluate the composition of intestinal microbiota in four groups of mice: mice without treatment (n = 3), mice treated with 2% dextran sodium sulfate (DSS) in the drinking water (n = 4), mice treated with polyinosinic-polycytidylic acid (poly (I:C)) (n = 5), and mice treated with both DSS and poly (I:C) (n = 6). The relative bacterial abundance is shown at the species level. Results are expressed as the mean ± SE.

Supplementary Figure 6. Compositional alterations of intestinal microbiota in the stool of mice treated with polyinosinic-polycytidylic acid and/or dextran sodium sulfate. Stool samples were subjected to 16S rRNA sequencing to evaluate the composition of intestinal microbiota in four groups of mice: mice without treatment (n = 3), mice treated with 2% dextran sodium sulfate (DSS) in the drinking water (n = 4), mice treated with polyinosinic-polycytidylic acid (poly (I:C)) (n = 5), and mice treated with both DSS and poly (I:C) (n = 6). The relative bacterial abundance is shown at the species level. Results are expressed as the mean ± SE.

Supplementary Figure 7. Production of IFN-α and IL-33 by pancreatic plasmacytoid dendritic cells isolated from the mice treated with both dextran sodium sulfate and polyinosinic-polycytidylic acid. Plasmacytoid dendritic cells (pDCs) were identified as PDCA-$1^{+}B220^{low}$ cells and FACS-sorted. pDCs ($5x10^{5}$/mL) were stimulated with *Staphylococcus aureus* and *Staphylococcus sciuri* at the indicated doses for 48 hrs. Cell culture supernatants were subjected to enzyme-linked immunosorbent assay to detect IFN-α and IL-33 as described in Figure 4. Expression levels of IFN-α and IL-33 in the culture supernatants were measured. Results are expressed as the mean ± SE. $^{**}P < 0.01$, n.s. (not significant).

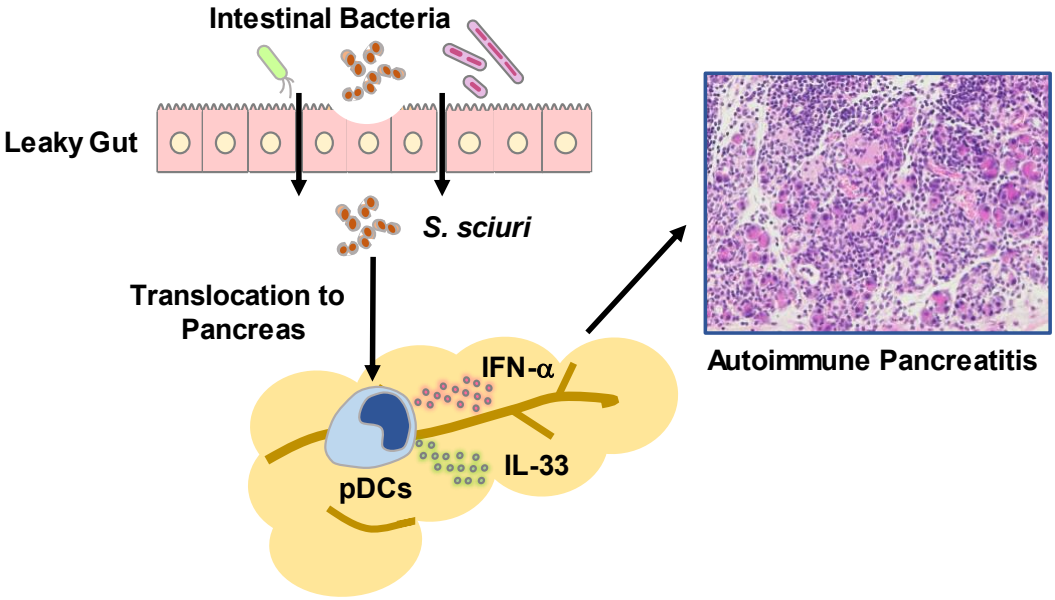

Graphical Abstract

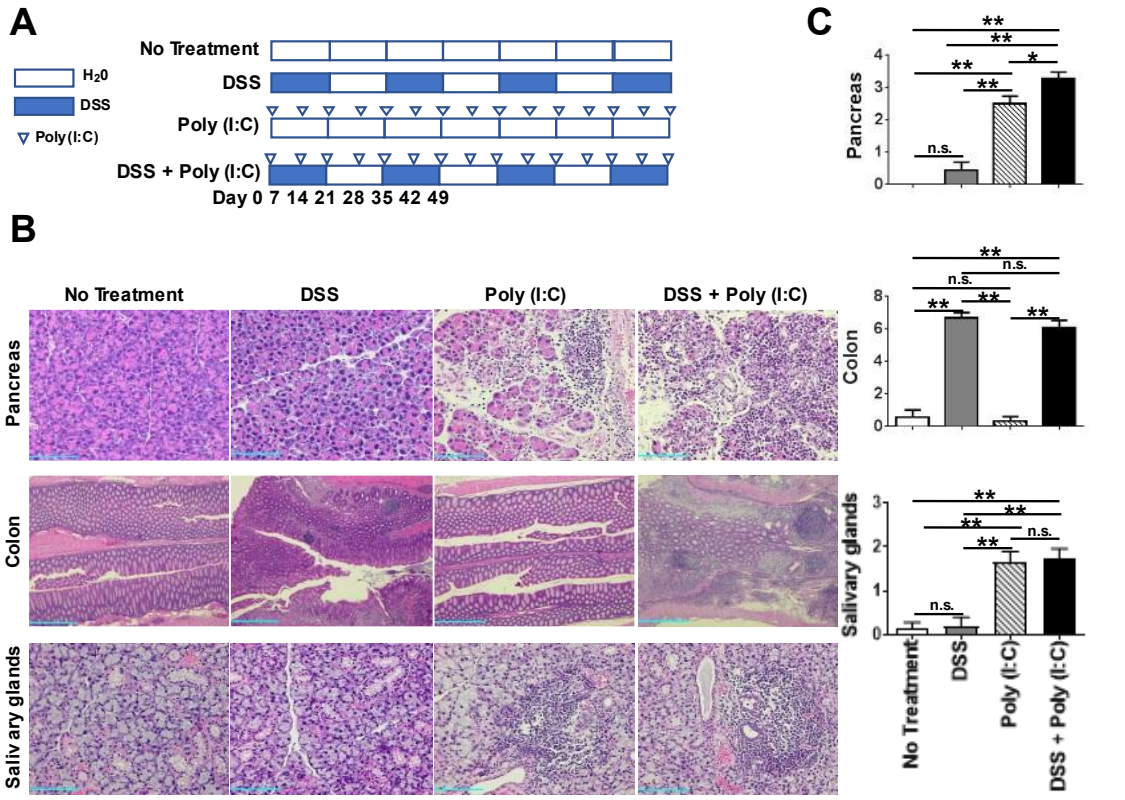
A
H20
DSS
Poly (I:C)
No Treatment
DSS
Poly (I:C)
DSS + Poly (I:C)
Day 0 7 14 21 28 35 42 49
B
No Treatment
DSS
Poly (I:C)
DSS + Poly (I:C)
Pancreas
Colon
Salivary glands
C
Pancreas
Colon
Salivary glands
n.s.
No Treatment
DSS
Poly (I:C)
DSS + Poly (I:C)

FIGURE 1

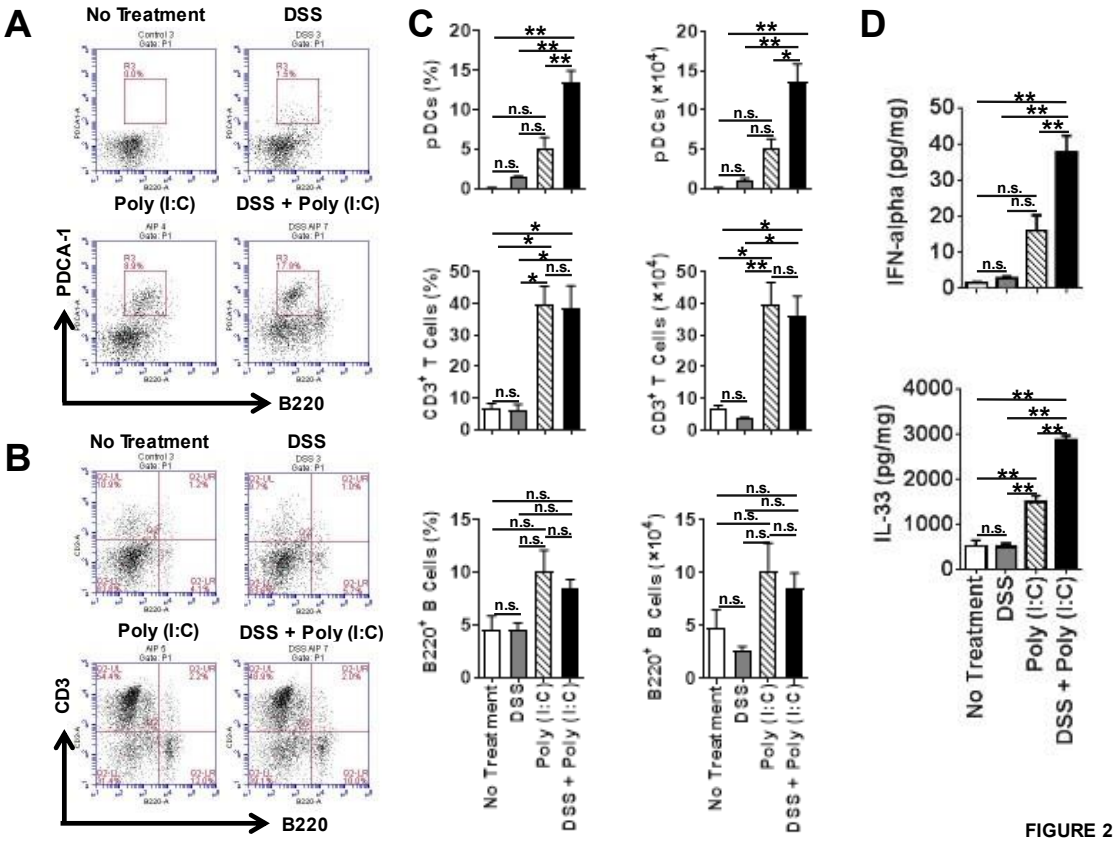
A
No Treatment
DSS
Poly (I:C)
DSS + Poly (I:C)
PDCA-1
B220
B
No Treatment
DSS
Poly (I:C)
DSS + Poly (I:C)
CD3
B220
C
pDCs (%)
pDCs (×10⁴)
CD3⁺ T Cells (%)
CD3⁺ T Cells (×10⁴)
B220⁺ B Cells (%)
B220⁺ B Cells (×10⁴)
n.s.
No Treatment
DSS
Poly (I:C)
DSS + Poly (I:C)
D
IFN-alpha (pg/mg)
IL-33 (pg/mg)
n.s.
No Treatment
DSS
Poly (I:C)
DSS + Poly (I:C)

FIGURE 2

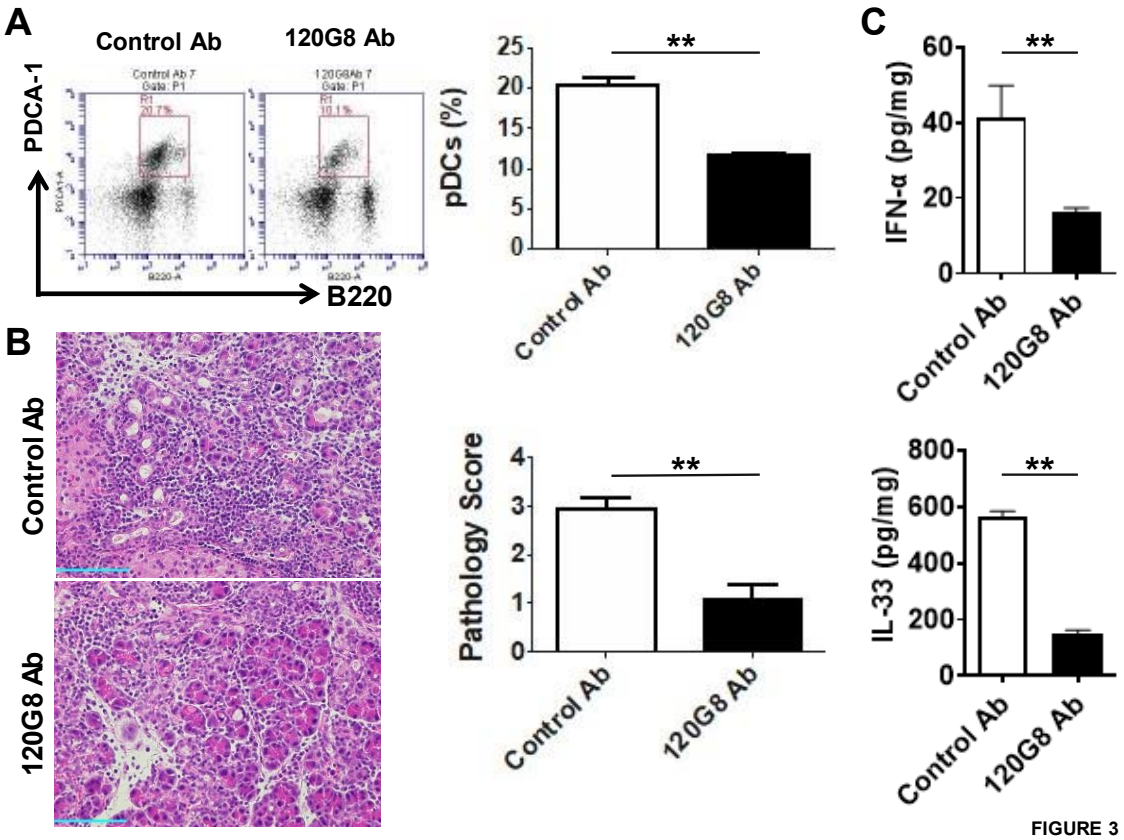
A
Control Ab
120G8 Ab
PDCA-1
B220
B
Control Ab
120G8 Ab
pDCs (%)
**
Control Ab
120G8 Ab
C
IFN-α (pg/mg)
**
Control Ab
120G8 Ab
Pathology Score
**
Control Ab
120G8 Ab
IL-33 (pg/mg)
**
Control Ab
120G8 Ab

FIGURE 3

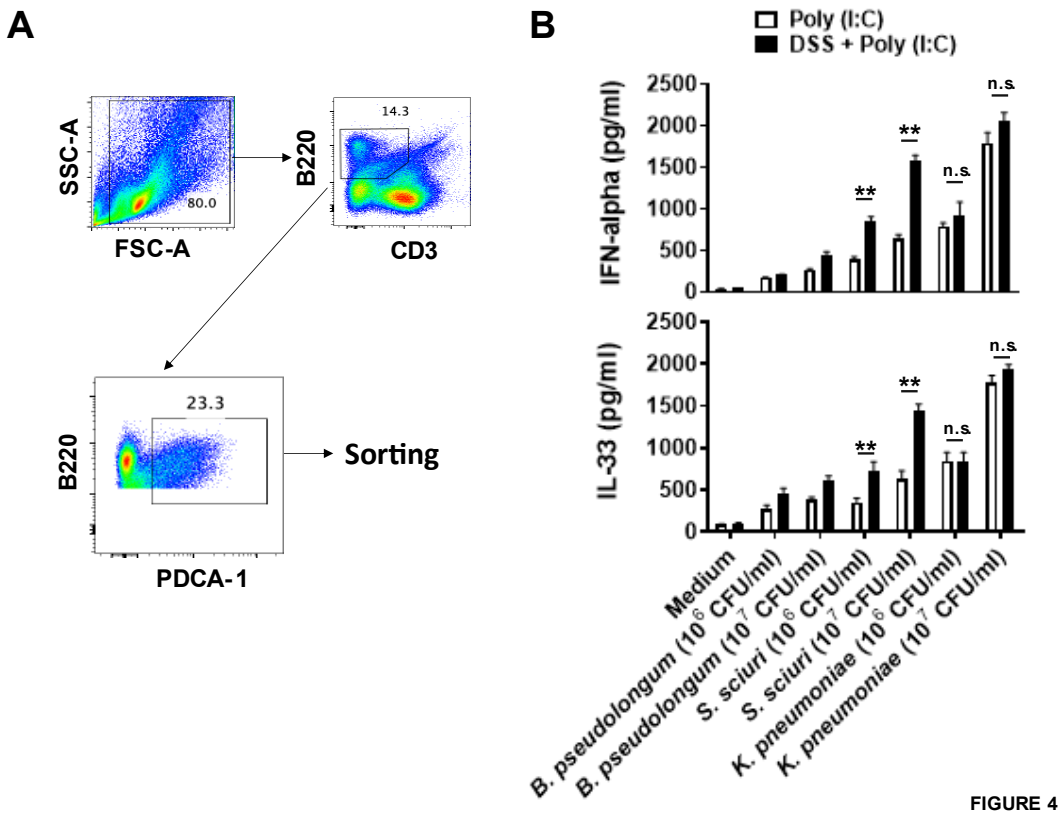
A
SSC-A
FSC-A
80.0
B220
CD3
14.3
B220
PDCA-1
23.3
Sorting
B
Poly (I:C)
DSS + Poly (I:C)
IFN-alpha (pg/ml)
IL-33 (pg/ml)
2500
2000
1500
1000
500
0
**
n.s.
Medium
B. pseudolongum (10^6 CFU/ml)
B. pseudolongum (10^7 CFU/ml)
S. sciuri (10^6 CFU/ml)
S. sciuri (10^7 CFU/ml)
K. pneumoniae (10^6 CFU/ml)
K. pneumoniae (10^7 CFU/ml)

FIGURE 4

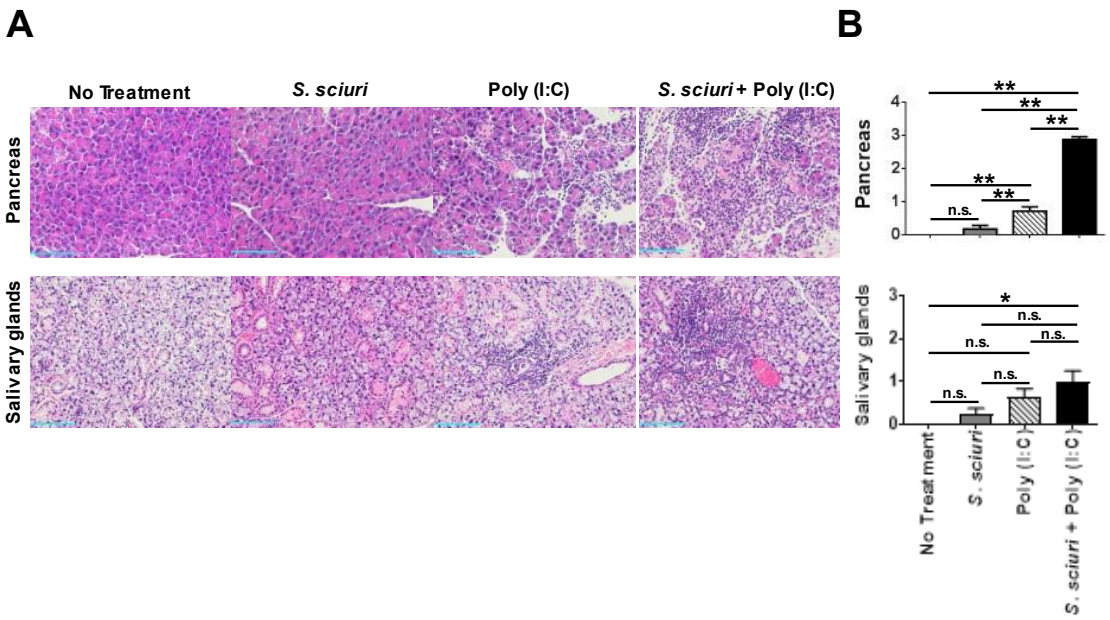
A
B
No Treatment
S. sciuri
Poly (I:C)
S. sciuri + Poly (I:C)
Pancreas
Salivary glands
n.s.
**
*
No Treatment
S. sciuri
Poly (I:C)
S. sciuri + Poly (I:C)

FIGURE 5

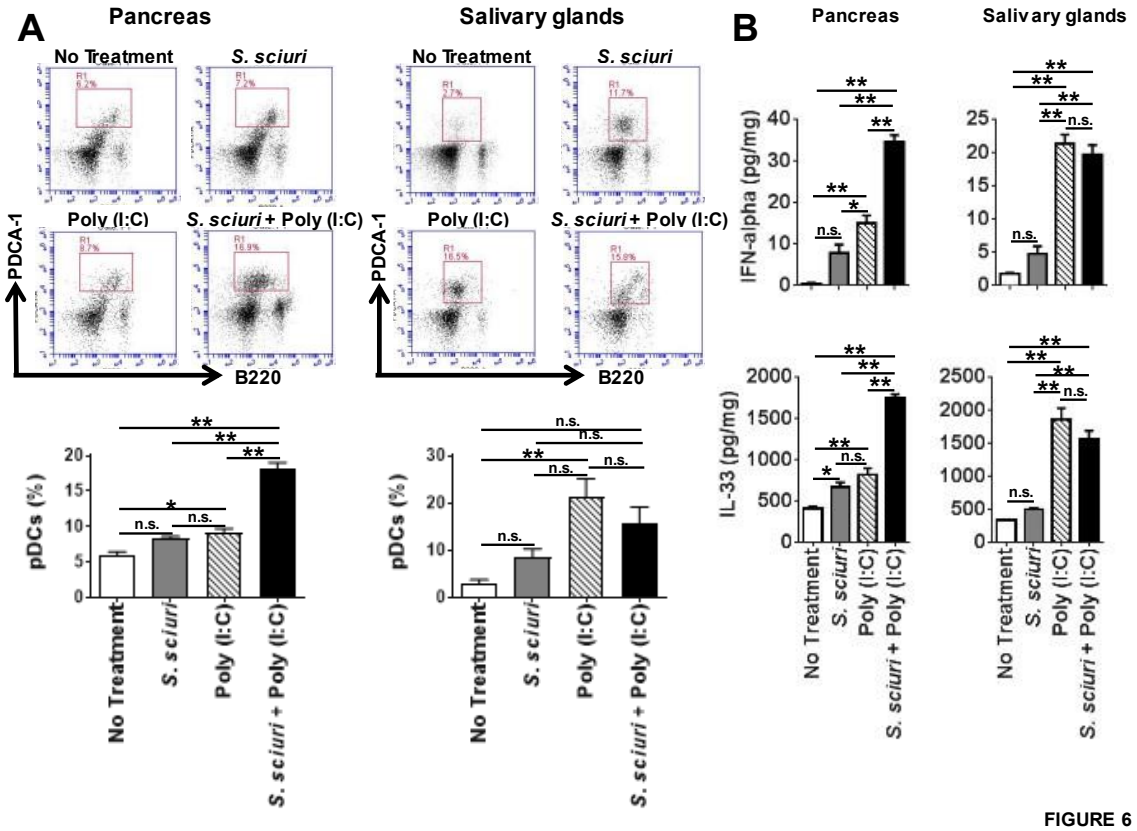
A
Pancreas
Salivary glands
No Treatment
S. sciuri
Poly (I:C)
S. sciuri + Poly (I:C)
PDCA-1
B220
pDCs (%)
B
IFN-alpha (pg/mg)
IL-33 (pg/mg)
n.s.

FIGURE 6

SUPPLEMENTARY FIGURE 1

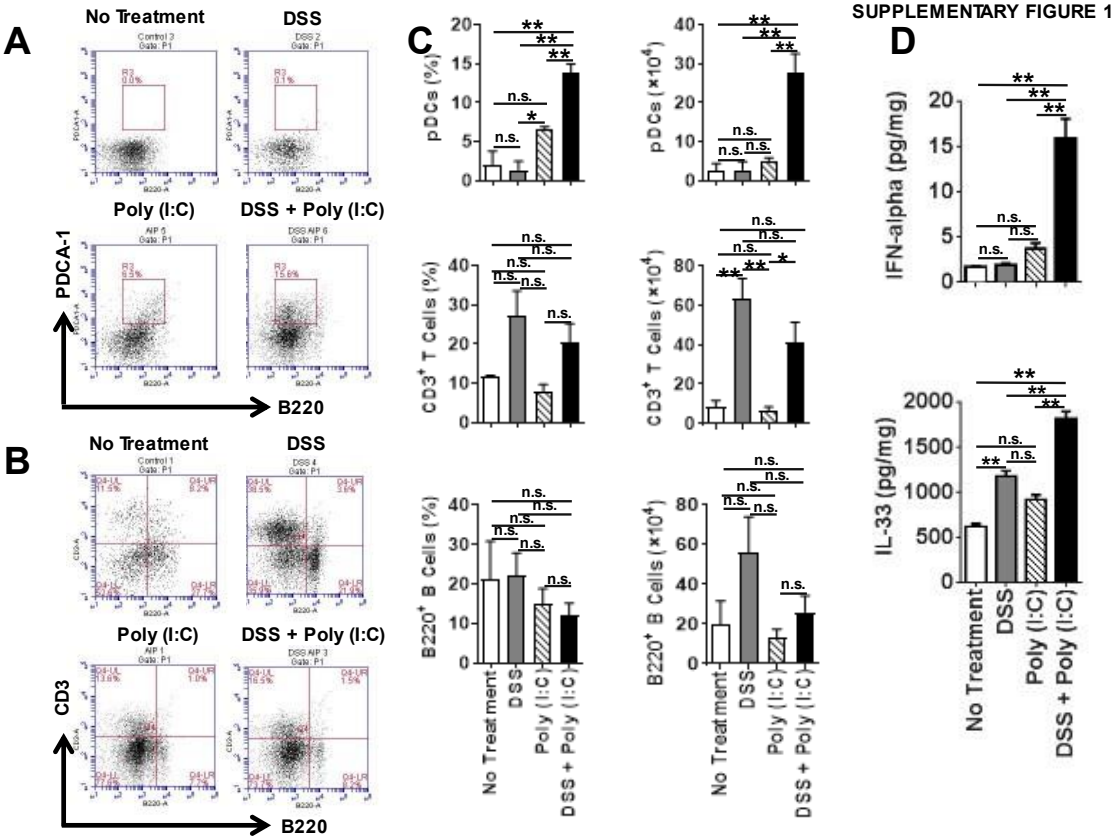

SUPPLEMENTARY FIGURE 2

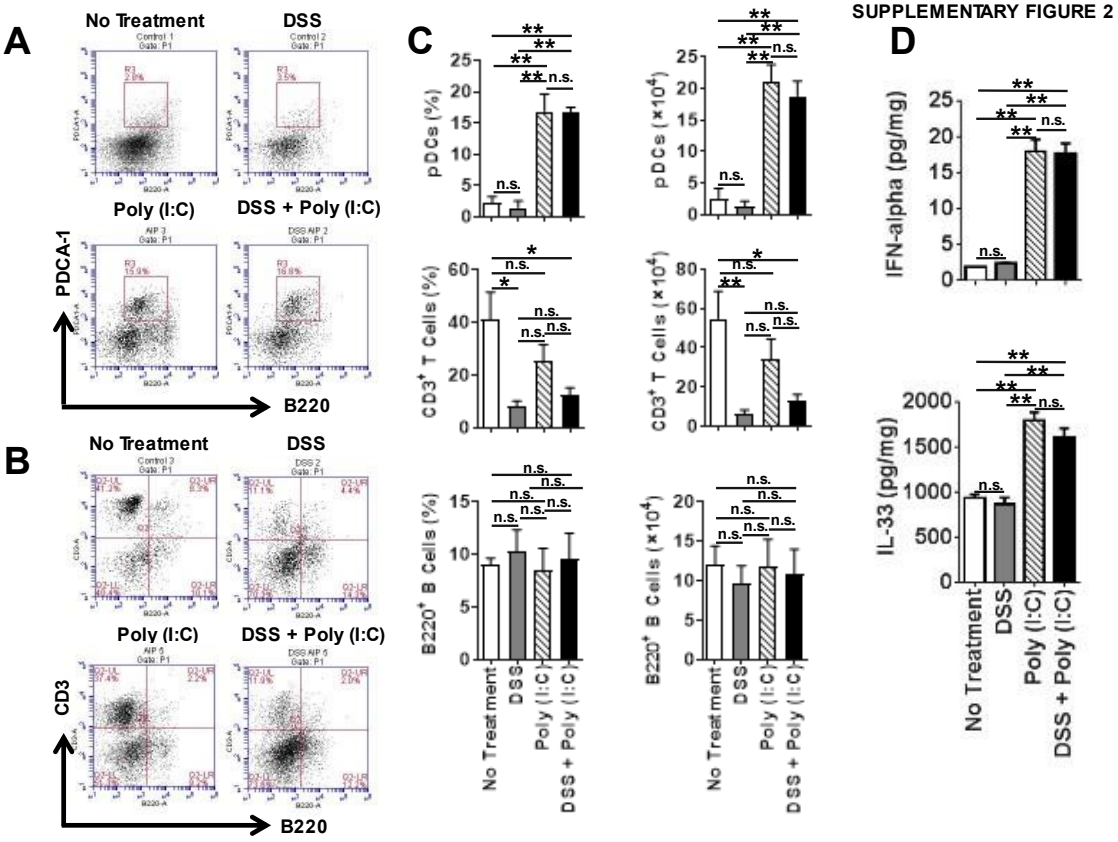

SUPPLEMENTARY FIGURE 3

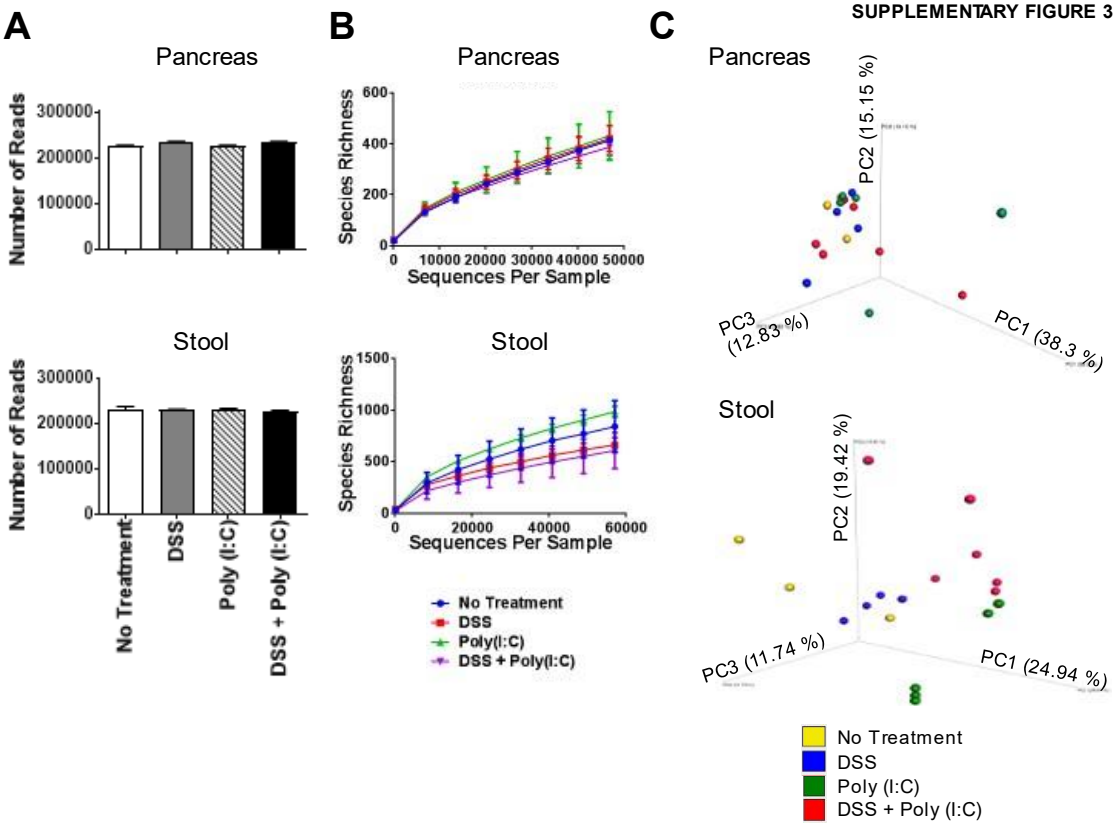

SUPPLEMENTARY FIGURE 4

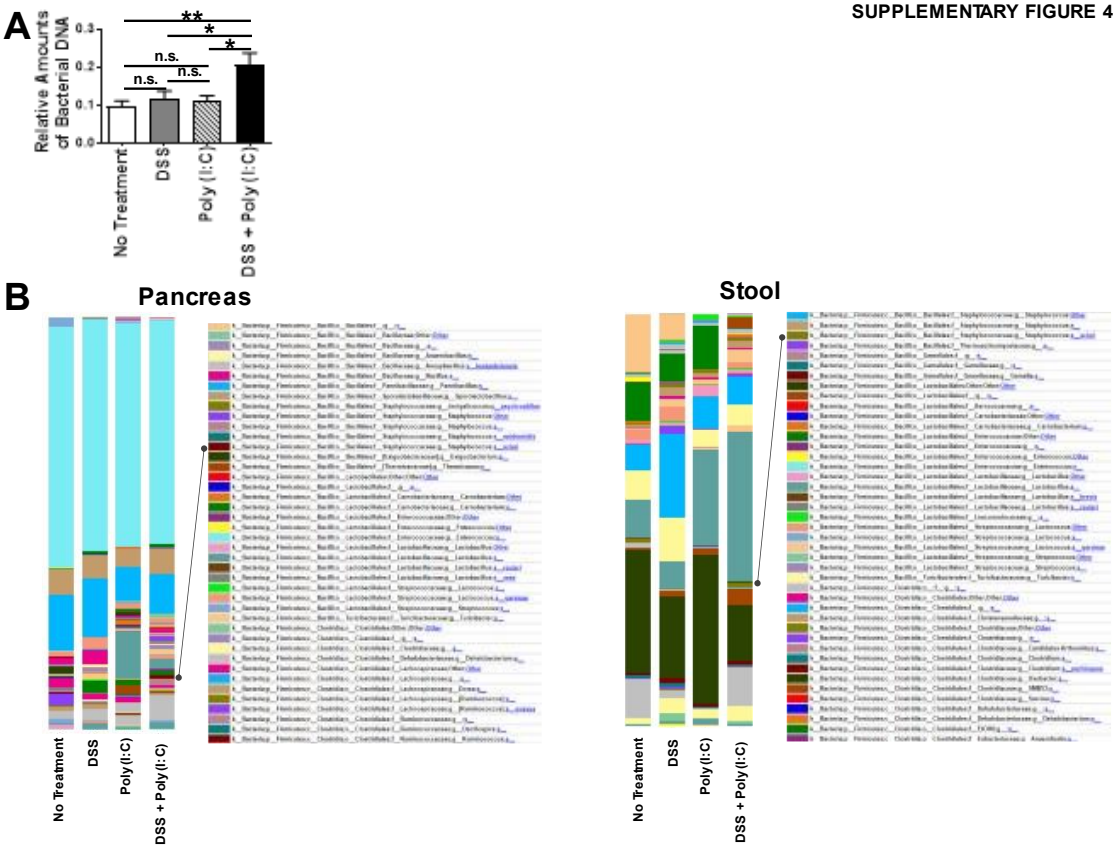

SUPPLEMENTARY FIGURE 5

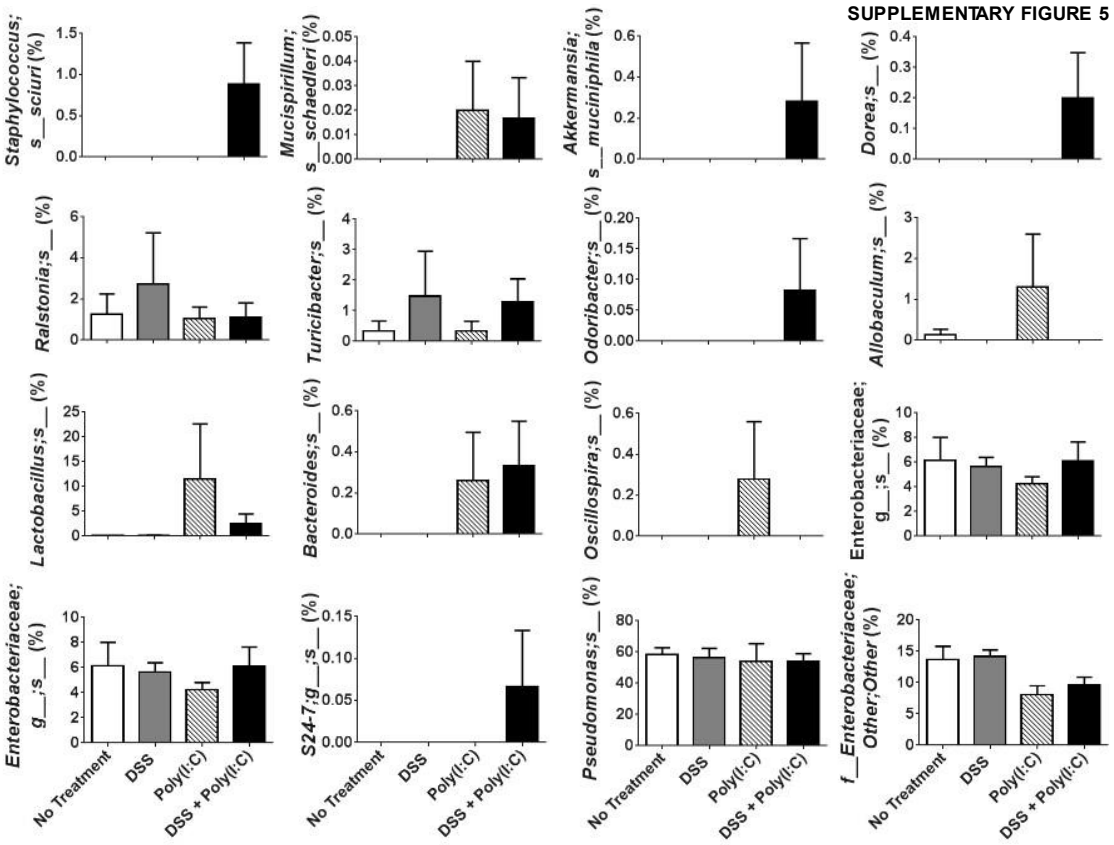

SUPPLEMENTARY FIGURE 6